

Document downloaded from:

<http://hdl.handle.net/10251/163285>

This paper must be cited as:

Ferri, J.; Llinares Llopis, R.; Moreno, J.; Lidon-Roger, JV.; Garcia-Breijo, E. (2020). An investigation into the fabrication parameters of screen-printed capacitive sensors on e-textiles. *Textile Research Journal*. 90(15-16):1749-1769.
<https://doi.org/10.1177/0040517519901016>



The final publication is available at

<https://doi.org/10.1177/0040517519901016>

Copyright SAGE Publications

Additional Information

Corresponding Author:

Jose Ferri. Textile Research Institute (AITEEX), Alicante, Spain.

Email: josue.ferri@aitex.es

Impact of textile substrates, conductive and dielectric inks on capacitive sensors for e-textiles

Josue Ferri^{1,3}, Raúl Llinares Llopis³, Jorge Moreno¹, Jose Vicente Lidón-Roger² and Eduardo Garcia-Breijo²

¹ Textile Research Institute (AITEEX), Alicante 03801, Spain; josue.ferri@aitex.es; jmoreno@aitex.es.

² Instituto Interuniversitario de Investigación de Reconocimiento Molecular y Desarrollo Tecnológico (IDM), Universitat Politècnica de València, Universitat de València, Valencia 46022, Spain; jvlidon@eln.upv.es; egarciab@eln.upv.es.

³ Departamento de Comunicaciones, Universitat Politècnica de València, Alcoy 03801, Spain; joferpa1@dcom.upv.es; rllinares@dcom.upv.es.

Abstract

The development of sensors based on conductive and dielectric inks integrated on textiles requires the knowledge of the parameters that influence on printing process, as well as the characteristics that the textile provides to the sensor. Dielectric inks are usually used to obtain the capacitive sensor, but in this work, a textile has been used directly as the dielectric part. Thus, the same textiles influence sensitively on the value of the permittivity and the thickness of the dielectric of the capacitor, two fundamental parameters on the estimation of its capacity. On the other hand, the choice of the conductive ink, its viscosity features, solid content, as well as printing parameters, such as printing direction, also impacts on the way of obtaining the electrodes of the capacitive sensor, a less important parameter for the estimation of the capacity, but determinant to select the fabrics that can be printed. This work studies the influence of fabrics, inks and printing parameters to print a capacitor on a textile. The results will contribute to smart textile applications based on projected capacitive technologies. The experiments carried out on different fabrics and inks have provided results with capacities of less than 60 pF, the limit where the sensors based on capacitive technologies are located.

Keywords

Printed electronic, screen-printing, capacitive sensors, touchpad, wearables

Smart textiles, also known as electronic textiles or e-textiles, are fabrics that can sense or react to the external environment, producing a designed and useful response [1,2,3]. The features of smart textiles, such as flexibility and conformability to the human body, allow them to be used in diverse applications. Healthcare [4,5], Sports [5,6], Military [7] or Gaming [8,9] are some of the fields where smart textiles can be employed.

Smart textiles consist of sensors, a data processing unit and, and optionally, actuators. The sensors are the essential elements for smart textiles, and they are usually embedded into the fabric. The data processing unit is usually implemented with microcontrollers measuring different parameters depending on the manufacturer. Regarding the actuators, several types can be found. Some of them include materials that change their colour when the temperature change [10], vibrators that respond to external stimuli [11,12] or electroluminescent displays [13,14].

Two main sensing technologies can be found in smart textiles. The first one uses resistive sensors and is based on the measurement of the variation of the electrical resistance of a conductive structure. It has been successfully applied to measure pressure [15], respiration [16] or temperature [17]. The second technology employs capacitive sensors, relying on the measurement of the capacitance of at addressable electrodes. Applications such as humidity [18], electromyography [19] or touch sensors [20] make use of capacitive sensors. This latter technology provides some advantages, such as a high linearity, low hysteresis, and fast response time, enable to use it in real-life applications [21].

Focus on capacitive touch sensors two broad categories can be found: surface capacitive technology and projected capacitive technology. Projected capacitive technology is regarded as the most popular technology for touch sensors [22], permits a higher resolution and features that make them ideal for industrial or outdoor applications [23]. There are two types of touch sensing signal acquisition used in projected capacitive technology. The widely used one is mutual-capacitive sensing since it can detect multi-touch positions [22]. On the other hand, self-capacitance provides a fast system response time. Although there are controllers that support only one type, there are others which offer both self-capacitance and mutual-capacitance types.

Capacitive sensors use electrode structures and multilayer electrode structures conforming capacitors. The simplest structure of a capacitor consists of two conductors, normally two conductive plates, also named electrodes, separated by an insulator, a dielectric layer. The capacitance of the resulting capacitor depends basically on three parameters: the area of the surface of the conductive plates, the distance between the plates, given by the resulting thickness of the insulating layer, and the relative permittivity or dielectric constant of the insulating material. The capacitance can be controlled considering that it is directly proportional to the area of the plates and the relative permittivity, and inversely proportional to the distance between the plates. One important parameter to be considered regarding the electrodes is the obtained resistivity, or its reciprocal, the conductivity. According to the conductivity of the electrodes, when the resistivity increases, the mobility of the electrodes decrease, and this will reduce the system sensitivity [24,25].

Different techniques can be used to implement the electrodes on a textile surface. Some designs are based on conductive columns and rows that can be simply drawn onto opposite sides of a piece of insulating material using a conductive ink. Another different approach is to use alternating conductive and isolating threads that are glued on the opposite sides of the textile substrate [26]. Sputtering processes can also be used to form high resolution circuits on fabrics with different types of capacitors such as two parallel plates, interdigital or stretchable planar electrodes [27,28]. There also exist implementations where the electronic capabilities are integrated into fiber-based sensors via coating processes on the fiber conforming a dielectric layer sandwiched between two parallel conductive surfaces [29,30]. Among all the existing technologies, the thick planar printing process with screen printing technology of conductive inks is the most used. It is due to the fact that it can produce entire electronic circuits on a planar fabric board at once and can also re-produce the identical circuit boards repeatedly. In addition, this system can be easily converted into roll to roll production, resulting in a low cost and high productivity system [27,31,32].

Regarding the dielectric layer, it is usually implemented with dielectric inks, although previous research works showed how a fabric surface can be used as the dielectric layer in an array structure of capacitive sensors obtaining a dynamic range of 100 fF - 10 pF with a pixel pitch of 8 mm [24]. In the design it is important take into consideration that the dielectric permittivity in textile materials can have small variations, due to the fact that depends on factors such as the working frequency, temperature, moisture, and packing density [33].

The resulting capacitance of the sensor must fit the requirements of the microcontroller used. Most of the commercial circuits use a square wave signal as a reference, and measure the differences of the reference signal respect to the signal received from the capacitor affected by the change of the capacitance. The working frequency have a direct relation with the capacitance, the range selected being the most suitable for the sensors in combination with the circuit. Circuits such as FMA1127 from Fujitsu, implement a maximum clock frequency of 20 kHz and a minimum one of 1.25 kHz, requiring a capacitance load of 400 pF for a standard mode and 40 pF for a fast mode [34]. PCF8883 and PCF8885 from NXP work with a capacitance range between 10 pF to 60 pF, and frequencies between 56 to 112 kHz [35]. In [13], the microcontroller used was MTCH6102 from Microchip [13,20] that works optimally with up to 60 pF (30 pF typically).

This paper shows the behaviour and influence of different smart textile materials used as a part of a capacitor printed using screen printing technology. The work is divided in two different parts, one corresponding to simple conducting printed solutions and the other one to an implementation of a flat capacitor. The conductive experiments used different types of conductive inks printed on several textile fabrics. The resistance and conductivity for different inks and fabrics were measured considering several factors such as printed shape orientation, printing direction or ink viscosity. This work also addresses the problem of printing conductive inks on high roughness fabrics, offering solutions that minimize the

problems of conductivity. The solutions are based on a preliminary printing of a dielectric ink layer or on the use of heat-sealed polyurethane films. The permittivity and thickness of the materials used was analysed, allowing to carry out a theoretical analysis of the capacitance in function of the used materials. Finally, the work presents an implementation of a capacitor structure according to the analysed materials, evaluating the impact of the different elements into the capacitance values.

Materials and method

Materials

For the first part of the work, in order to evaluate the behaviour of different fabrics as dielectrics, a selection of the most commonly used materials with different thicknesses were made. Different cotton, polyester and mixed fabrics with different fabric densities, thread diameters and weaves have been used. Tables 1 and 2 show the main characteristics of the fabrics used.

Although there are not specific conductive inks to be applied on textiles, different conductive inks were selected considering high conductivities and stretchability properties for printing electronics on flexible substrates. The used conductive inks (Table 3) are made of silver with different characteristics of solid contents, viscosities, flexibility and stretchability. All of them were inks for screen-printing: PE873 from DUPONT, 127-48 from CREATIVE, HPS-DEV FLX5 from NOVACENTRIC and IPC-603X from INKRON.

For the second part of the experiment, three dielectric inks (Table 4), with the flexibility and stretchability characteristics shown in the table, were used. The inks were 127-48D from CREATIVE, DI-7542 from EMS and IPD-670 from INKRON. These inks were selected considering that were compatible with the selected conductive inks and were suitable for being used on flexible substrates for printing electronics.

For the third part of the work, four polyurethane films (Table 5) were used. The films were UE50 from DESLTAR, EU94DS from DELSTARD, 2370 from INSPIRE and UAF-445 from ADHESIVE FILMS. The films were selected considering that they had a good adhesion to the fabrics using a low temperature and a good behaviour against shrinking.

Finally, for the last part of the work, a selection of the utilized inks, fabrics and polyurethane films was made to implement a capacitor to measure its capacity.

Table 1. Fabric characteristics (I): composition and ligament.

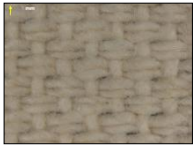




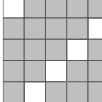
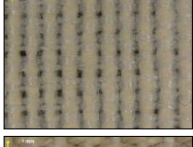
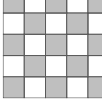
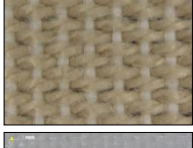
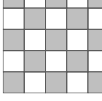
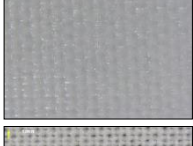
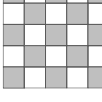

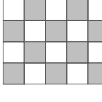

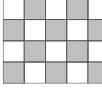
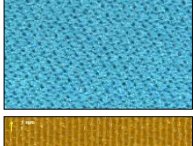

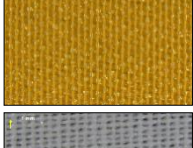
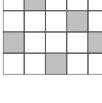
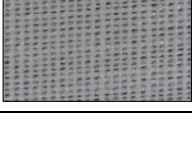
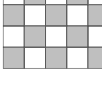
| Fabric | Picture | Weft Material | Warp Material | Ligament |
|--|---|---------------|---------------|---|
| Type A 100 % Cotton |  | Cotton | Cotton | Teleton  |
| Type B 100 % Cotton |  | Cotton | Cotton | Teleton  |
| Type C 100 % Cotton |  | Cotton | Cotton | Twill  |
| Type D 50% Cotton 50% Polyester |  | Cotton | Polyester | Taffeta  |
| Type E 100% Polyester |  | Polyester | Polyester | Taffeta  |
| Type F 100% Polyester |  | Polyester | Polyester | Taffeta  |
| Type G 100% Cotton Waterproof |  | Cotton | Cotton | Taffeta  |
| Type H 100% Cotton |  | Cotton | Cotton | Taffeta  |
| Type I 100% Polyester/ Thermoplastic Polyurethane (TPU) |  | Polyester | Polyester | Knitted weave  |
| Type J 100% Polyester |  | Polyester | Polyester | satin 4/1  |
| Type K 60% Cotton 40% Polyester |  | Polyester | Cotton | Taffeta  |

Table 2. Fabric characteristics (II): size and weight characteristics.

| Fabric | Weft Density (Thread/cm) | Warp Density (Thread/cm) | Fabric Density (Thread/cm ²) | Wire Weft Diameter (μm) | Wire Warp Diameter (μm) | Thickness (μm) | Grammage (g/m ²) |
|--------|--------------------------|--------------------------|--|-------------------------|-------------------------|----------------|------------------------------|
| Type A | 10 | 28 | 38 | 400 | 400 | 530±10 | 312±5 |
| Type B | 7 | 24 | 31 | 450 | 450 | 700±19 | 324±2 |
| Type C | 26 | 34 | 60 | 300 | 300 | 470±20 | 235±2 |
| Type D | 13 | 26 | 39 | 450 | 450 | 380±7 | 181±1 |
| Type E | 10 | 22 | 32 | 350 | 350 | 570±11 | 226±4 |
| Type F | 24 | 38 | 62 | 300 | 300 | 110±8 | 112±4 |
| Type G | 32 | 44 | 76 | 160 | 160 | 130±5 | 115±6 |
| Type H | 44 | 32 | 76 | 220 | 220 | 190±2 | 118±1 |
| Type I | - | - | - | 130 | 130 | 270±9 | 148±3 |
| Type J | 40 | 40 | 80 | 70 | 120 | 210±10 | 135±2 |
| Type K | 28 | 48 | 76 | 200 | 200 | 200±8 | 104±1 |

Table 3. Silver inks characteristics.

| | DUPONT PE873 | CREATIVE 127-48 | NOVACENTRIC HPS-DEV FLX5 | INKRON IPC-603X |
|-----------------------------------|--|--|---|---|
| Sheet Resistivity (mΩ/sq/mil) | <75 | 25 | 230 | <15 |
| Solids (%) | 60-65 | >82 | 72.6 (82.7) | 100 |
| Viscosity (Pas) | 50-80 @0.2 s ⁻¹ | 26-30 | 28 @0.1 s ⁻¹ | 16 @0.25 s ⁻¹ |
| Screens polyester (threads /inch) | 120-77 | | 400-80 | |
| Curing | 160° C – 10 min | 125° C – 30 min | 160° C – 10 min | 130° C – 15 min |
| Properties | <ul style="list-style-type: none"> • Stretchable • Flexible • Washable with encapsulation | <ul style="list-style-type: none"> • Flexible • Washable | <ul style="list-style-type: none"> • Flexible • Washable • Water-based | <ul style="list-style-type: none"> • High Stretchability • Flexible |

Table 4. Dielectric inks characteristics.

| | CREATIVE 127-48D | EMS DI-7542 | INKRON IPD-670 |
|----------------------------------|--|---|---|
| Viscosity (Pas) | 15-20 | 7 @0.05 s ⁻¹ | 32 @2.5 s ⁻¹ |
| Screens polyester [threads/inch] | | 156-305 | |
| Curing | 125° C – 60 min | 0.5 J/cm ² | 130° C – 15 min |
| Properties | <ul style="list-style-type: none"> • Flexible | <ul style="list-style-type: none"> • Flexible • UV-Cure | <ul style="list-style-type: none"> • Stretchable |

Table 5. Polyurethanes characteristics.

| | DELSTAR EU50 | DELSTAR EU94DS | INSPIRE 2370 | ADHESIVE FIMS UAF-445 |
|---|--------------|----------------|--------------|-----------------------|
| Thickness (μm) | 50 | 80 | 30 | 120 |
| Weight (g/m ³) | 55 | 94 | 57 | - |
| MVTR* upright (g/m ² /24 hours)@37°C | 700 | 400 | 118 | - |
| Tensile Strength MD** (gf/cm) | 1200 | 3000 | 65 | - |
| Elongation at break MD** (%) | 1000 | 700 | 65 | 450 |

* Moisture vapor transmission rate (MVTR)

**Machine direction (MD)

Manufacturing

The used manufacturing technology was based on the serigraphic technology of thick film. The screen-printing process consists of forcing pastes of different characteristics over a substrate through some screens using squeegees. Openings in the screen define the pattern that will be printed on the substrate by serigraphy. The final thickness of the pastes can be adjusted by varying the thickness of the screens.

In order to test the conductive inks on the fabrics, a design with different geometries, sizes and orientations was made (Figure 1). In order to compare the different results, the pattern contained shapes named as SX, where S varies 1 to 23, for instance, S1 refers to a thin circular shape.

When screen-printing technology is used, it is necessary to manufacture frames with a screen mesh for the design. The screen for the conductors was a 230 mesh polyester material (PET 1500 90/230-48 from Sefar) and the screen for the dielectric layer, when needed, was a 76 mesh polyester material (PET 1500 30/76-120 PW from Sefar). Afterwards, to transfer the pattern to the screen mesh, a UV film Dirasol 132 from Fujifilm was used. The final screen thickness was 74 μm for the screen for the conductors and 217 μm for the screen for the dielectrics. The pattern was transferred to the screen by using a UV light source unit IC-5000 from BCB.

Printing was carried out using an EKRA E2XL screen-printer with a shore of 75° hardness squeegee, 60° squeegee angle, 1 mm snap-off, 3.5 bar force, and 100 mm/s.

After the deposition of the inks, these were cured in a FED-115 air oven from BINDER at 130° C for 15 minutes in order to use the same curing characteristics for all inks. Although some of the brands recommends curing at higher temperatures, the temperature can be lower increasing the curing time. On the other hand, the fabrics suffer deterioration at high temperatures. Consequently, in order to prevent the deterioration of the textile, the curing temperature was fixed to 130°C for all the inks. All the inks except DI-7542 can be cured with air oven. In the case of the dielectric ink DI-7542 from EMS, a Ncure-Lab/Static 120 UV oven from EneMaq was used with 0.5 J/cm².

The polyurethanes were thermosealed on the fabrics with a heatpress DCH-100 from Microtec at 130° C for 60 seconds.

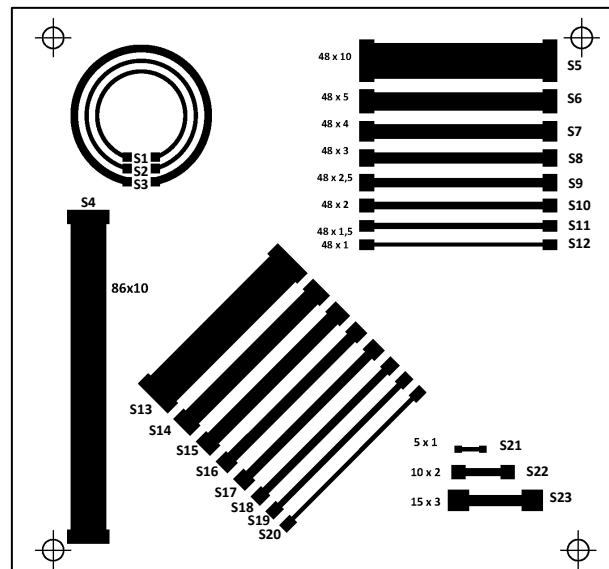


Figure 1. Pattern design with different geometries, sizes and orientations to test conductive inks on fabrics.

Experimental setup

An experimental setup in several phases was designed with the objective of studying the influence of the materials on the capacitive sensors developed on textiles. The initial challenge was to achieve a good conductivity on the textile substrate using the selected conductive inks. For this purpose, the pattern

shown in Figure 1 was used combining all the inks with all the fabrics selected in the three first phases of the work. In those cases where the conductivity was not good enough, solutions were sought to improve the conductivity of the conductive ink printed flattening the textile surface. Finally, the challenge was to evaluate different materials in order to obtain a fixed and controlled capacity. In this sense, as a goal, a capacity of less than 60 pF was set, making the obtained result suitable to be used in capacitive based sensor applications.

The first phase was to screen-print the different types of the silver conductive inks shown in Table 3 on the different fabrics shown in Tables 1 and 2 to assess the behaviour of the conductive inks on the fabrics and thus to determine in which type of fabrics these inks can be directly printed on or in which ones a preconditioning of the fabric surface is necessary.

The second phase was to screen print the different dielectric inks shown in Table 4 with the aim of improving the conditions of the screen printing of the conductive inks in those cases that were necessary. As some fabric surfaces are not flat enough, it was considered to print a layer with dielectric ink before printing the conductive pattern. In addition, this phase allowed to study the influence of the whole dielectric formed by the fabric and the printed dielectric layer on the relative permittivity. Moreover, the obtained thickness and its influence on the capacitance value were evaluated.

The third phase consisted of performing the same procedure as in phase two, but using the polyurethane films shown in Table 5. With the same purpose of flattening the fabric surface, a polyurethane film was attached on the fabric surface before printing the conductive pattern. For this case, the relative permittivity and thickness variable were able to be more controlled than using the dielectric ink.

The last phase allowed to assess the capacitance value of a capacitor implemented using each of the materials utilized in the previous different experiments. The conductive plates were made printing an area of silver material on both faces of the fabric perfectly aligned between them; the thickness of the dielectric varied according to the type of material used. When needed, the textile surface was flattened using the solutions exposed. The structure used in this part is presented in Figure 25.

Experimental procedure

Previous to the screen printing, a thermic treatment was applied to all the fabrics to avoid variations of size due to the curing temperature of the inks. The thermic treatment applied consisted of introducing the fabrics in an oven at 130° C for 15 minutes. After that, the roughness and thickness of the fabrics were measured to be used in a further analysis. Moreover, an extra substrate was included as a reference. The selected reference substrate was a transparent PET (polyethylene terephthalate), due to the fact that is commonly used in printing electronics and has a good flat surface.

The design shown in Figure 1 was printed with the different inks in order to measure the thickness of the ink printed and the resistance in each sample. In addition, a calculation of the resistance was done considering the datasheet of the ink to be compared with the measured resistance.

For the first phase, the design shown in Figure 1 that includes several patterns with different geometries, sizes and orientations (shapes), was screen printed to test the conductive inks on the fabrics. The printing was carried out in three directions, one according to the weft (named of 0°), other one according to the warp (named of 90°) and the last one of 45°. For each fabric, four inks were used. The procedure started with a first printing with two ink passes and a curing of 130° for 15 minutes, measuring the value of resistance of each pattern. Then, a second extra printing with other two ink passes was performed with the same type of curing as previously to have better conductivity performance. After this printing, the values of resistance of the patterns were measured again. With these measures, an assessment of the behaviour of the inks on the different fabrics was conducted in function of the direction of printing, pattern orientation, features of the fabric (composition, density, weave, thickness of the fabric and diameter of the thread) and viscosity and solid content of the inks.

For the second phase, only those fabrics that did not lead to conductive patterns due to the characteristics of their surface were used. Therefore, it was necessary to set up the surface of the fabrics with the printing of dielectric inks. For each fabric, three dielectric inks were used. The procedure started with a first printing with two dielectric ink passes and a curing of 130° for 15 minutes. Next, a second printing with other two dielectric ink passes was performed with the same type of curing as previously.

Lastly, two printings with two conductive ink passes were performed with a curing of 130° for 15 minutes, this time only according to the weft direction. After this printing, the values of resistance of the patterns were measured. With these measures, an assessment of the behaviour of the dielectric inks, as well as of the conductive inks, on the different fabrics was conducted.

On the third phase, the dielectric inks were substituted by polyurethanes since they have suitable dielectric features and their thickness is constant. Moreover, they can be added to the textile in an easy way through heat seal. Four polyurethanes heat sealed at 130° for 60 seconds were used. Next, two printings with two conductive ink passes were performed with a curing of 130° for 15 minutes, according to the weft direction. After this printing, the values of resistance of the patterns were measured. With these measures, an assessment of the behaviour of the polyurethane films, as well as of the conductive ink, on the different fabrics was conducted. Since the mechanical behaviour of the polyurethane on the fabric must have the minimal influence, an additional study of stretching of the polyurethane films was carried out, using silver square draws with 1 mm width and 10 mm height screen printed on the polyurethane. Since there were fabrics that did not allow more than 10% of elongation, each pattern was stretched between 1% and 10% of length and then, the resistance values were measured for each case.

On the last phase, a printing of flat capacitors was performed varying the type of fabric and ink to assess the value of the capacity obtained in function of the used materials. For this phase, the thickness and the relative permittivity of the materials used were measured as well.

Measurements

The resistance measurements were made with a FLUKE 8845A multimeter. The capacitance between electrodes was measured at 100 kHz with a KEYSIGHT U1733C LCR meter.

The relative permittivity (ϵ_r) measures were made with a Hewlett Packard 4263A LCR meter. The following measurement accessories were used: Hewlett Packard 16089B Kelvin Clips Leads and a Yokogama-Hewlett Packard 16451A Dielectric Test Adaptor. The LCR meter was configured to measure a tension level of 1V, with an average of 64 samples and a low read rate (Level = 1 V, Avg = 64, Meas Time = Low). The measurement mode was Cp and D (parallel capacity and loss tangent). The capacity measurements were taken at three different parts of the fabric with a 4-frequency scan (0.1 kHz, 1 kHz, 10 kHz y 100 kHz). The ϵ_r value was obtained directly from the Cp value.

The measurements of the thickness of the fabric were taken at 4 different points using a Mitutoyo CP calibre CD-6'' with a 10 μ m resolution.

The roughness measurements were taken with a Mitutoyo SurfTest SJ-410 roughness tester using the standard ISO1997. For the roughness profile (R), a gaussian filter was used (Gauss) with a measurement section of 8 mm ($\lambda_c = 8$ mm) for 2 sections (N=2), the needle of the tester going across 16 mm. The parameters Ra (Arithmetic mean of roughness), Rq (Mean square of roughness) and Rz (Rmax) were measured.

The 3D profilometry was measured with a Filmetrics Profilm3D profilometer with a Nikon CF IC Epi Plan x 20 objective.

Regarding images, high resolution topographic images by SE (Secondary Electrons) and maps of crystalline and textural orientations by EBSD (Electron Backscatter Diffraction) were taken with the ZEISS ULTRA 55 Scanning Electron Microscope Field Emission Gun (FE-SEM). Macroscopic images were taken with a LEICA MZ APO stereomicroscope.

For the tensile test, an INSTRON equipment was used. It allows to determine the behaviour of materials under axial stretching loads. As previously stated, the length of the sample was increased between 1% and 10% of its nominal length and its resistance was measured in each case.

Results and discussion

Study of the conductive inks on fabrics

In the first phase, the silver inks were screen printed on the fabrics. Previously, a printing on a plastic substrate (PET) was carried out to have a resistance value reference for each of the inks. The obtained resistance values for each shape and ink are shown in Table 6. For the sake of clarity, a letter has been added to the sample: Letter C indicates circumference, H horizontal, V vertical and D diagonal orientation.

Table 6. Resistance (Ω) of the samples for each silver ink on a PET substrate after the second printing with two passes per printing. Letter C indicates circumference, H horizontal, V vertical and D diagonal orientation.

| | DUPONT PE873 | CREATIVE 127-48 | NOVACENTRIC HPS-DEV FLX5 | INKRON IPC-603X |
|-------|-----------------|--------------------|-----------------------------|--------------------|
| S1-C | 6.70±0.10 | 3.30±0.25 | 10.28±0.45 | 1.97±0.08 |
| S2-C | 8.31±0.53 | 4.20±0.55 | 13.69±0.86 | 2.45±0.21 |
| S3-C | 5.52±0.81 | 2.80±0.21 | 9.64±0.56 | 1.68±0.15 |
| S4-V | 1.45±0.08 | 0.67±0.01 | 1.50±0.20 | 0.47±0.01 |
| S5-H | 1.05±0.02 | 0.59±0.05 | 1.27±0.10 | 0.32±0.04 |
| S6-H | 1.52±0.11 | 0.81±0.02 | 2.13±0.15 | 0.45±0.01 |
| S7-H | 1.91±0.09 | 0.92±0.02 | 2.50±0.21 | 0.54±0.10 |
| S8-H | 2.30±0.20 | 1.28±0.04 | 2.94±0.18 | 0.67±0.07 |
| S9-H | 2.80±0.31 | 1.33±0.10 | 3.55±0.35 | 0.76±0.04 |
| S10-H | 3.32±0.10 | 1.63±0.09 | 4.19±0.11 | 0.84±0.07 |
| S11-H | 4.23±0.15 | 1.99±0.01 | 5.40±0.10 | 1.04±0.12 |
| S12-H | 6.21±0.73 | 2.83±0.03 | 7.18±0.10 | 1.35±0.21 |
| S13-D | 0.94±0.05 | 0.50±0.01 | 1.12±0.05 | 0.33±0.02 |
| S14-D | 1.62±0.12 | 0.77±0.01 | 1.97±0.17 | 0.47±0.02 |
| S15-D | 1.81±0.21 | 0.92±0.04 | 2.43±0.21 | 0.55±0.01 |
| S16-D | 2.35±0.15 | 1.06±0.03 | 3.08±0.31 | 0.66±0.07 |
| S17-D | 2.83±0.10 | 1.23±0.10 | 3.61±0.20 | 0.77±0.01 |
| S18-D | 3.10±0.20 | 1.49±0.15 | 4.53±0.08 | 0.90±0.06 |
| S19-D | 4.01±0.11 | 1.80±0.05 | 5.72±0.56 | 1.26±0.11 |
| S20-D | 5.82±0.20 | 2.50±0.68 | 7.26±0.35 | 1.62±0.06 |
| S21-H | 1.01±0.05 | 0.54±0.01 | 1.30±0.08 | 0.31±0.02 |
| S22-H | 1.10±0.08 | 0.51±0.01 | 1.41±0.05 | 0.35±0.01 |
| S23-H | 1.10±0.10 | 0.52±0.01 | 1.36±0.05 | 0.35±0.01 |

In order to double check the obtained values, the resistance was calculated considering the sheet resistivity given by the manufacturer (Table 3). For this calculation, the layer thickness obtained for each ink was measured.

The average thickness on the PET substrate for DUPONT PE873 is 1.2 μm , for CREATIVE 127-48 is 4.3 μm , for NOVACENTRIC HPS-DEV FLX5 is 10 μm and for INKRON IPC-603X is 7 μm .

The thickness of the conductor layer before drying can be calculated using Equation 1:

$$T_{bd} = (T_S \cdot A_S) + T_f \quad (1)$$

where T_{bd} is the conductor thickness before drying, T_S is the screen thickness, A_S is the open area of screen and T_f is the photo-sensitive film thickness. With the values from the datasheet of the screen used for the conductors that was 230 mesh polyester material (PET 1500 90/230-48 from Sefar) and the UV film Dirasol 132 from Fujifilm, the obtained value for T_{bd} was 21.75 μm ($T_S=71 \mu\text{m}$, $A_S=25\%$ and $T_f=4 \mu\text{m}$)

T_{bd} is reduced after drying according to the % of solid content and the ink solvent type. For the DUPONT ink, the reduction after drying was 94.5%, for the CREATIVE ink 80.2%, for the NOVACENTRIC ink 54% and for the INKRON ink 67.8%.

Next, the value of the real resistivity was calculated and compared with the sheet resistivity provided by the manufacturer. Equations 2 and 3 allow to carry out the comparison:

$$R_{SX} = \rho \frac{L}{t \cdot W} \rightarrow \rho = \frac{R_{SX} \cdot t \cdot W}{L} \quad (2)$$

$$\rho_{sheet} = \frac{\rho}{25 \mu m} \quad (3)$$

where R_{Sx} is the resistance of sample Sx , ρ is the resistivity, ρ_{sheet} is the sheet resistivity from the manufacturer, t is the layer thickness, L is the length and W the width of the resistance. The $25 \mu m$ value is the print thickness used by the manufacturers to specify the sheet resistivity.

Thus, for the ink DUPONT PE873, the resultant sheet resistivity is $7.5 \text{ m}\Omega/\text{sq}/\text{mil}$ (according to the manufacturer $< 75 \text{ m}\Omega/\text{sq}/\text{mil}$), for the ink CREATIVE 127-48, the resultant sheet resistivity is $12.5 \text{ m}\Omega/\text{sq}/\text{mil}$ (according to the manufacturer $< 25 \text{ m}\Omega/\text{sq}/\text{mil}$), for the ink NOVACENTRIC HPS-DEV FLX5, the resultant sheet resistivity is $80.6 \text{ m}\Omega/\text{sq}/\text{mil}$ (according to the manufacturer $< 230 \text{ m}\Omega/\text{sq}/\text{mil}$) and for the ink INKRON IPC-603X, the resultant sheet resistivity is $16 \text{ m}\Omega/\text{sq}/\text{mil}$ (according to the manufacturer $< 15 \text{ m}\Omega/\text{sq}/\text{mil}$).

Once the inks were characterised, they were printed on the fabrics as stated on the experimental procedure. The obtained results showed that not all fabrics were able to be screen printed. For the screen printable fabrics, the results depended on factors such as the shape orientation, printing direction, type of material or ink viscosity. Table 7 shows the printing results for all the fabrics in percentage of the number of samples that present conductivity against those samples that present open circuit (infinite impedance). The table shows the percentage in function of the number of printings made and of the orientation of the printing. The orientation and size of the shape have been jointly considered for the sake of simplicity.

Table 7. Percentage of samples (%) that show conductivity after the first and second impression depending on the inks and fabrics. The orientation of the drawing and its size have been considered globally in order to simplify the table.

| | DUPONT PE873 | | | | | | CREATIVE 127-48 | | | | | | NOVACENTRIC HPS-DEV FLX5 | | | | | | INKRON IPC-603X | | | | | | | |
|--------|-----------------|-----------------|-----------------|-----------------|-----------------|-----------------|--------------------|-----------------|-----------------|-----------------|-----------------|-----------------|-----------------------------|-----------------|-----------------|-----------------|-----------------|-----------------|--------------------|-----------------|-----------------|-----------------|-----------------|-----------------|-----|---|
| | 0° | | 45° | | 90° | | 0° | | 45° | | 90° | | 0° | | 45° | | 90° | | 0° | | 45° | | 90° | | | |
| | 1 st | 2 nd | 1 st | 2 nd | 1 st | 2 nd | 1 st | 2 nd | 1 st | 2 nd | 1 st | 2 nd | 1 st | 2 nd | 1 st | 2 nd | 1 st | 2 nd | 1 st | 2 nd | 1 st | 2 nd | 1 st | 2 nd | | |
| Type A | 0 | 0 | 0 | 0 | 0 | 4 | 0 | 0 | 0 | 0 | 0 | 0 | 0 | 0 | 8 | 0 | 34 | 0 | 8 | 0 | 13 | 4 | 34 | 13 | 39 | |
| Type B | 0 | 0 | 0 | 0 | 0 | 0 | 0 | 0 | 0 | 0 | 0 | 0 | 0 | 0 | 0 | 0 | 8 | 0 | 0 | 0 | 0 | 17 | 0 | 34 | 0 | 0 |
| Type C | 22 | 44 | 0 | 4 | 0 | 17 | 44 | 56 | 0 | 52 | 0 | 65 | 65 | 74 | 8 | 52 | 39 | 74 | 78 | 95 | 52 | 82 | 13 | 82 | | |
| Type D | 4 | 4 | 0 | 0 | 0 | 52 | 4 | 4 | 0 | 4 | 0 | 87 | 4 | 4 | 0 | 8 | 0 | 48 | 4 | 4 | 0 | 0 | 47 | 52 | | |
| Type E | 0 | 0 | 0 | 0 | 0 | 0 | 0 | 0 | 0 | 0 | 0 | 0 | 0 | 0 | 0 | 0 | 0 | 0 | 0 | 0 | 0 | 0 | 0 | 0 | 0 | |
| Type F | 100 | 100 | 100 | 100 | 100 | 100 | 100 | 100 | 100 | 100 | 100 | 100 | 0 | 100 | 0 | 100 | 0 | 87 | 100 | 100 | 100 | 100 | 100 | 100 | 100 | |
| Type G | 82 | 100 | 100 | 100 | 100 | 100 | 70 | 78 | 61 | 70 | 61 | 70 | 0 | 78 | 0 | 48 | 0 | 91 | 100 | 100 | 100 | 100 | 100 | 100 | 100 | |
| Type H | 74 | 100 | 76 | 91 | 61 | 91 | 70 | 78 | 56 | 74 | 56 | 65 | 69 | 82 | 60 | 78 | 56 | 78 | 100 | 100 | 87 | 87 | 87 | 95 | | |
| Type I | 74 | 91 | 74 | 78 | 78 | 87 | 87 | 100 | 78 | 87 | 78 | 87 | 22 | 74 | 0 | 30 | 8 | 69 | 100 | 100 | 100 | 100 | 82 | 95 | | |
| Type J | 9 | 30 | 17 | 52 | 7 | 78 | 0 | 0 | 0 | 0 | 0 | 0 | 4 | 4 | 30 | 70 | 13 | 30 | 73 | 82 | 82 | 87 | 91 | 100 | | |
| Type K | 82 | 100 | 87 | 87 | 87 | 87 | 52 | 65 | 39 | 48 | 39 | 74 | 0 | 9 | 0 | 0 | 0 | 4 | 78 | 100 | 95 | 95 | 100 | 100 | | |

Fabrics type A, B, C, D and E had problems with the printing for any ink and any orientation. Fabric C showed better results with the INKRON ink but not achieving optimal results. Fabrics type F, G, H and I showed the best results, with a higher percentage for the case of INKRON ink. Fabric J only presented results with INKRON ink for certain printing orientations. Fabric K only showed good percentages with DUPONT and INKRON inks.

When there was conduction on the samples, it appeared from the first printing, and only in a few cases it improved after the second printing. This allowed to obtain good results with only one printing.

Studying the results in terms of the composition of the fabrics, no conclusive results could be found. This is due to the fact that for the cotton fabrics (A, B, C, G y H), the printing was not correct for some of them (A, B and C) and for G and H, it depended on the ink used (more optimal for DUPONT and INKRON inks). For the polyester fabrics (E, F and J), the behaviour was the same. Fabric F had a high conductivity percentage, whereas fabrics E and J had low percentages. The mixture fabrics (D and K) followed the same behaviour, fabric D has low percentages rather than K that has high conductivity for DUPONT and INKRON inks.

Regarding the type of weft, it neither did it influence on the results. Thus, with Teleton (A and B) the results were low, with Taffeta (D, E, F, G, H and K) were dissimilar and with twill (C) the result was low as well.

The thickness of the fabric and the diameter of the thread seemed to have influence on the printing. Fabrics with less than 300 μm of thickness (F, G, H, I, J and K) showed better results than thicker fabrics (A, B, C, D and E). The relation was similar considering the diameter of the thread, finding better results for thread diameters lower than 200 μm (F, H, I, J and K). Taking into account a similar parameter, the thread count per area, fabrics A, B, D and E, with a lower thread count per area (< 40 threads/ cm^2), presented worse results than those with a higher thread count per area. The fabric C is a remarkable case. It had a thickness of 470 μm and a thread diameter of 300 μm , but with a thread count per area of 60 threads/ cm^2 . This fabric presented the best results over the rest of the thick fabrics, confirming the influence of the thread count.

The thread diameter and the thread count influenced on the roughness of the fabric as shown in Table 8. Thus, the fabrics with a Ra value lower than 25 μm showed a better behaviour regarding to the printing.

Table 8. Parameters of fabrics' roughness.

| | Ra (μm) | Rq (μm) | Rz (μm) |
|--------|--------------------------------------|--------------------------------------|--------------------------------------|
| Type A | 32.23 | 39.67 | 186.55 |
| Type B | 52.94 | 64.01 | 274.63 |
| Type C | 28.58 | 34.78 | 166.08 |
| Type D | 52.46 | 65.91 | 249.19 |
| Type E | 46.92 | 55.06 | 246.01 |
| Type F | 5.16 | 6.28 | 30.53 |
| Type G | 15.83 | 19.41 | 113.04 |
| Type H | 16.78 | 20.77 | 110.40 |
| Type I | 16.52 | 20.90 | 113.22 |
| Type J | 24.26 | 29.09 | 148.30 |
| Type K | 14.71 | 18.26 | 109.65 |

Regarding the ink viscosity, INKRON ink with a lower viscosity (16 Pas) seemed to have the best conduction rate on fabrics F, G, H, I, J and K. Instead, CREATIVE and NOVACENTRIC inks with a similar viscosity (≈ 26 Pas), provided different results, CREATIVE being the one that presented better rates. This could be explained considering the type of solvent used (not provided by the manufacturer). In this sense, DUPONT ink, with a higher viscosity (50 Pas), showed better rates on some fabrics than CREATIVE or NOVACENTRIC.

To determine the behaviour of the ink in each fabric, the values of resistance for the different shapes were measured in each case. Table 9 shows the value of the resistance of the most significant shapes (in this case, the ones with higher size) in function of the type of fabric, shape orientation, printing direction and inks. The measure of the value of the resistance was taken after the second printing. Looking at the roughness of the fabrics, two groups can be differentiated: from type A to E, that were the roughest ones, and from type F to K, that were the less rough ones. This different groups can also be obtained looking at the thickness of the fabric and the warp diameters. It is interesting to highlight that although all the printings using different directions were done with the same conditions, the results show that depending on the orientation of the shape, the resistance took higher or lower value. This effect is produced due to the fact that the threads on the surface behave as walls when the orientation of the threads does not coincide with the printing direction.

Table 9. Resistance value (Ω) of the most significant samples (larger size) depending on the fabrics, sample orientation, direction of the printing (0° same direction as the weft, 90° same direction as the warp and 45° diagonally to both) and inks. The measurement is made after the second printing. The measurement of infinite impedance (there is no conductivity) has been omitted to facilitate the reading of the table.

| | | DUPONT PE873 | | | CREATIVE 127-48 | | | NOVACENTRIC HPS-DEV FLX5 | | | INKRON IPC-603X | | |
|--------|-------|-----------------|------------|------------|--------------------|------------|------------|-----------------------------|------------|------------|--------------------|------------|------------|
| | | 0° | 45° | 90° | 0° | 45° | 90° | 0° | 45° | 90° | 0° | 45° | 90° |
| Type_A | S3-C | - | - | - | - | - | - | - | - | - | - | - | - |
| | S4-V | - | - | - | - | - | - | - | 223 | 76 | 56 | 116 | 3.1 |
| | S5-H | - | - | - | - | - | - | - | 450 | - | 14 | 270 | 0.4 |
| | S13-D | - | - | - | - | - | - | 147 | 376 | 133 | - | 95 | 2.5 |
| Type B | S3-C | - | - | - | - | - | - | - | - | - | - | - | - |
| | S4-V | - | - | - | - | - | - | - | - | - | - | 1.5 | - |
| | S5-H | - | - | - | - | - | - | - | - | - | 60 | 0.9 | - |
| | S13-D | - | - | - | - | - | - | - | - | - | - | 2.9 | - |
| Type C | S3-C | - | - | - | - | - | - | - | - | - | 2.6 | 25 | - |
| | S4-V | 2.5 | 265 | 21.2 | 4.7 | 10 | 4.2 | 1.5 | 8.9 | 17.2 | 0.5 | 0.5 | 3.8 |
| | S5-H | 7.9 | - | - | 3.2 | 114 | 3.4 | 3 | 34.4 | 22.4 | 0.3 | 0.5 | 0.9 |
| | S13-D | 42.6 | - | - | 4.3 | 12.5 | 2 | 2 | 15.3 | 13.8 | 0.3 | 0.4 | 0.9 |
| Type D | S3-C | - | - | - | - | - | - | - | - | - | - | - | - |
| | S4-V | 3.4 | - | - | 2.7 | - | - | 6.7 | 450 | - | 5 | - | 2.6 |
| | S5-H | - | - | 9.3 | - | 199 | 2.4 | - | 640 | 49 | - | - | 0.2 |
| | S13-D | - | - | - | - | - | - | - | - | 100 | - | - | - |
| Type E | S3-C | - | - | - | - | - | - | - | - | - | - | - | - |
| | S4-V | - | - | - | - | - | - | - | - | - | - | - | - |
| | S5-H | - | - | - | - | - | - | - | - | - | - | - | - |
| | S13-D | - | - | - | - | - | - | - | - | - | - | - | - |
| Type F | S3-C | 11.3 | 18.5 | 15.2 | 3.6 | 4 | 3.7 | 18.5 | 49.6 | - | 6.9 | 5 | 6.9 |
| | S4-V | 1.8 | 4.3 | 2.5 | 0.8 | 0.9 | 0.8 | 3.4 | 10.8 | 4.5 | 0.9 | 1 | 1.7 |
| | S5-H | 1.8 | 2.6 | 2.2 | 0.6 | 0.6 | 0.6 | 1.8 | 2.4 | 3.5 | 1.1 | 1.6 | 1.2 |
| | S13-D | 1.2 | 1.8 | 1.6 | 0.6 | 0.6 | 0.6 | 2.2 | 6.5 | 3.9 | 0.9 | 0.9 | 0.9 |
| Type G | S3-C | 4.6 | 3.9 | 2.8 | 5.7 | 21.6 | - | - | - | - | 1.3 | 1.3 | 1.6 |
| | S4-V | 0.8 | 0.6 | 0.6 | 0.5 | 1.7 | 3.2 | 11 | 742 | 1134 | 0.3 | 0.4 | 0.4 |
| | S5-H | 1 | 0.6 | 0.6 | 1 | 10.9 | 4.8 | 4 | 659 | - | 0.2 | 0.3 | 0.4 |
| | S13-D | 0.6 | 0.5 | 0.5 | 0.9 | 2.5 | 3.3 | 4.2 | 36 | - | 0.3 | 0.2 | 0.4 |
| Type H | S3-C | 35 | 38 | 54.8 | 13.5 | - | - | - | - | - | 1.6 | 5.4 | 1.7 |
| | S4-V | 2 | 1.9 | 2 | 0.8 | 1.1 | 0.8 | 8.6 | 10.7 | 7.2 | 0.3 | 0.4 | 0.3 |
| | S5-H | 1 | 2.5 | 2 | 0.6 | 1.9 | 2.1 | 2.5 | 86 | 13.7 | 0.3 | 0.3 | 0.3 |
| | S13-D | 1.1 | 1.1 | 1.6 | 0.6 | 0.7 | 1.5 | 3.6 | 7.5 | 3.6 | 0.3 | 0.3 | 0.3 |
| Type I | S3-C | 505 | 634 | 705 | 9.3 | 32.5 | 114 | - | - | - | 2.1 | 2 | 3.4 |
| | S4-V | 19.2 | 24.5 | 1.6 | 2 | 2.2 | 0.7 | 41.1 | 68 | 13.5 | 0.5 | 0.5 | 0.4 |
| | S5-H | 1.6 | 10.2 | 3.9 | 0.7 | 2.7 | 3.9 | 14.7 | 233 | 335 | 0.3 | 0.3 | 0.5 |
| | S13-D | 3.1 | 21.5 | 3.1 | 1 | 0.6 | 1.6 | 25.4 | 49 | 21.8 | 0.4 | 0.3 | 0.4 |
| Type J | S3-C | - | - | - | - | - | - | - | - | - | 12 | 1.7 | 1.8 |
| | S4-V | - | 33 | 133 | - | - | - | - | 124 | 43 | 0.7 | 0.3 | 0.3 |
| | S5-H | - | 301 | 7.4 | - | - | - | - | 12 | 90 | 0.3 | 0.4 | 0.2 |
| | S13-D | 10 | 3.9 | 3.5 | - | - | - | - | 17.5 | - | 0.7 | 0.2 | 0.2 |
| Type K | S3-C | 7.1 | - | - | - | - | - | - | - | - | 4.3 | 1 | 4.5 |
| | S4-V | 1 | 34 | 4 | 2.3 | 8.9 | 12.6 | 66 | - | 265 | 0.3 | 0.2 | 0.3 |
| | S5-H | 0.8 | 55 | 0.9 | 8.5 | 8.6 | 0.9 | 300 | - | - | 0.3 | 0.2 | 0.2 |
| | S13-D | 0.5 | 9.6 | 0.8 | 1.1 | 4.1 | 1.2 | - | - | - | 0.3 | 0.2 | 0.2 |

Table 9 allows to make a comparison based on the inks:

- DUPONT: As stated before, there was no conductivity on the shapes for fabrics A, B, C, D and E. For the fabrics with conductivity, a big variation in the results could be observed. In fabrics F, H, I, J and K, the resistance increased, whereas for fabric G the resistance diminished. This could imply that in fabric G, the obtained conductive layer thickness was greater than in the rest of fabrics, and it could be due to its waterproof treatment that improved the printing of this kind of ink. Regarding the printing directions, in general, the best results were obtained with 0° or 90° , whereas with the 45° direction, the obtained values were much higher. With fabrics F and H, similar values of resistance were obtained, but the printing direction had much influence on the obtained conductive layer thickness. In these cases, the optimal direction was 0° . Fabrics I and J

reported very high resistivity values, this could be due to the attainment of small thicknesses of the resulting conductive layer. With fabric K, reduced resistance values were only achieved with the printing direction 0° . It is worth noting the difficulty of achieving good results when printing circular elements, since very high resistance values were obtained. This implied very small ink thicknesses and the formation of different conductivity spaces through the circumference. This fact is possibly produced due to the change of orientation of the pattern with reference to the printing direction through the geometrical figure. Figure 2 shows an example where the resistance increased (Type F) or decreased (Type G). Notice that fabric F got a layer thickness lower than fabric G (zones delimited by a red line in the microscopic image, Figure 2.b). In the 3D profilometry (Figure 2.c), the difference of layer thickness can be observed. It is interesting to highlight that the ink in both cases was not uniform over the surface, but it acquired the form of the screen of the screen printing. This effect could be produced due to the fact that the fabrics retained the ink and did not allow it to flow laterally.

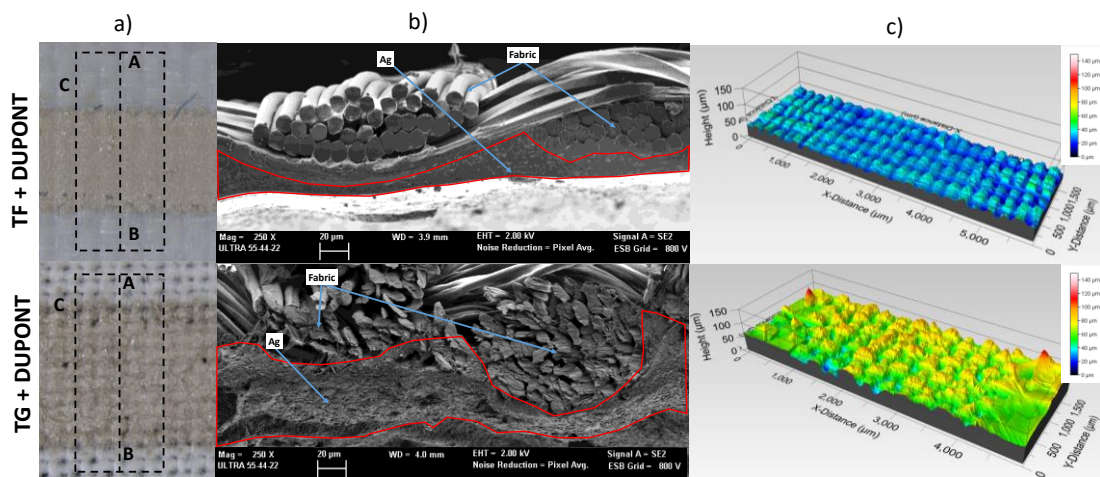


Figure 2. Fabrics type F y type G screen printed with DUPONT ink: a) Horizontal plane view (x8) of the fabrics, b) SEM micrograph showing device cross-section (A-B) where the fabric zone and the silver zone can be observed, c) 3D profilometry of the area C.

- **INKRON:** Its behaviour was excellent in most of the fabrics except in fabrics A, B, D and E. The obtained values were very similar for each shape in the three printing directions, even in the circular figures. In the case of fabric F, higher resistance values were obtained, due to a lower conductive layer thickness. Figure 3 shows the studied fabrics with the INKRON ink. Fabric F got a lower layer thickness. On the contrary, fabric G got a much higher thickness layer, even higher than the same case with DUPONT (zones delimited by a red line in the microscopic image, Figure 3.b). In the 3D profilometry (Figure 3.c), the difference of layer thickness can be observed. In this case, the ink seemed to be more uniform than in the case of DUPONT, this could be explained considering the lower viscosity of the INKRON ink.

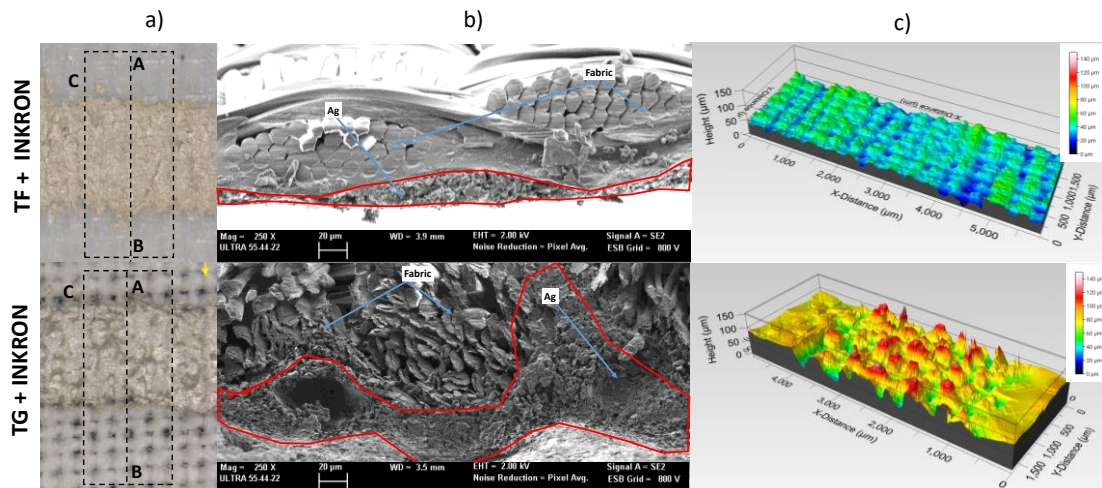


Figure 3. Fabrics type F and G screen printed with INKRON ink: a) Horizontal plane view (x8) of the fabrics, b) SEM micrograph showing device cross-section (A-B) where the fabric zone and the silver zone can be observed, c) 3D profilometry of the area C.

- CREATIVE: With this ink, the fabrics that got closer to the behaviour of the PET reference pattern were F and H, whereas fabrics G, I and K showed very dissimilar results. Once again, the circular shapes showed very high resistances, confirming the difficulty of achieving good results with this kind of figures.
- NOVACENTRIC: In general, for all the fabrics, results away from the PET reference pattern were obtained.

In general, it was observed that the printed ink distribution was not uniform. It could mainly depend on the way that the ink is absorbed in the fabric due to the structure of the same fabric and to the rheological characteristics of the ink. To assess the behaviour of the fabric in the smart textile, a SEM micrograph of each smart textile was taken. From Figure 4 to Figure 14, the SEM micrograph of each textile is shown, the top part corresponding to the DUPONT ink and the bottom part to the INKRON ink. The images on the left show the image by SE for a visual characterization of the textile and the ink, whereas the images on the right show the maps of crystalline and textural orientations by EBSD for a determination of the position of the silver particles. In these last images, the silver particles can be observed due to their white intensity with respect to the rest of the elements.

Figure 4 shows a magnification where the Ag flakes can be observed, on the DUPONT ink up to 10 μm and on the INKRON ink up to 15 μm . It is worth noting that the DUPONT ink has high viscosity and low solid content, whereas the INKRON ink has low viscosity and high solid content.

In Fabric A (Figure 4), the DUPONT ink was deposited forming a small layer on the ridges of the fabric and did not penetrate inside of the fabric. However, the INKRON ink deposited on the ridges as well as on the trenches of the fabric, penetrating inside of the fabric. With none of the two inks (neither with the rest), fiber wetting occurred. The ink only recoated the bundle of fibers that composed the thread of the weft and the warp. A similar situation could be observed with fabric B (Figure 5).

In fabric C (Figure 6), the DUPONT ink, as well as the INKRON ink, covered well the surface of the fabric and filled up the openings. For the case of the DUPONT ink, a lower quantity of silver was observed, possibly due to the viscosity, and hence, a lower conductivity was obtained when comparing to the INKRON ink in this fabric.

In fabric D (Figure 7), the inks had a very similar behaviour to that observed with fabric A.

The silver layer was very superficial (only on the ridges) in fabric E (Figure 8). The DUPONT and INKRON inks did not obtain a good conductivity. The inks did not penetrate in the fabric; possibly due to the fact that the fabric had some superficial finishing process not allowing the inks to penetrate.

In fabric F (Figure 9), both inks were perfectly screen printed; nevertheless, a higher quantity of silver was observed in the case of the INKRON ink. This possibly happened due to the higher amount of solids of this ink. Hence, the conductivities obtained with this fabric were better than those obtained with the INKRON ink.

Fabric G (Figure 10) showed a good compatibility with both inks which were well screen printed and penetrated deeply in the fabric. This fact was confirmed with the high conductivities obtained. The same happened with fabric H (Figure 11).

The behaviour of the inks in fabric I (Figure 12) was very similar to the observed in the fabric C.

In fabric J (Figure 13), the DUPONT ink hardly penetrated in the fabric, whereas the INKRON ink penetrated inside of the fabric. This behaviour could be due to the ink density and the shape of the ligament of this fabric.

Lastly, in fabric K (Figure 14), the two inks were well screen printed, but the best behaviour was observed in the case of the INKRON ink, agreeing with the resistance values obtained.

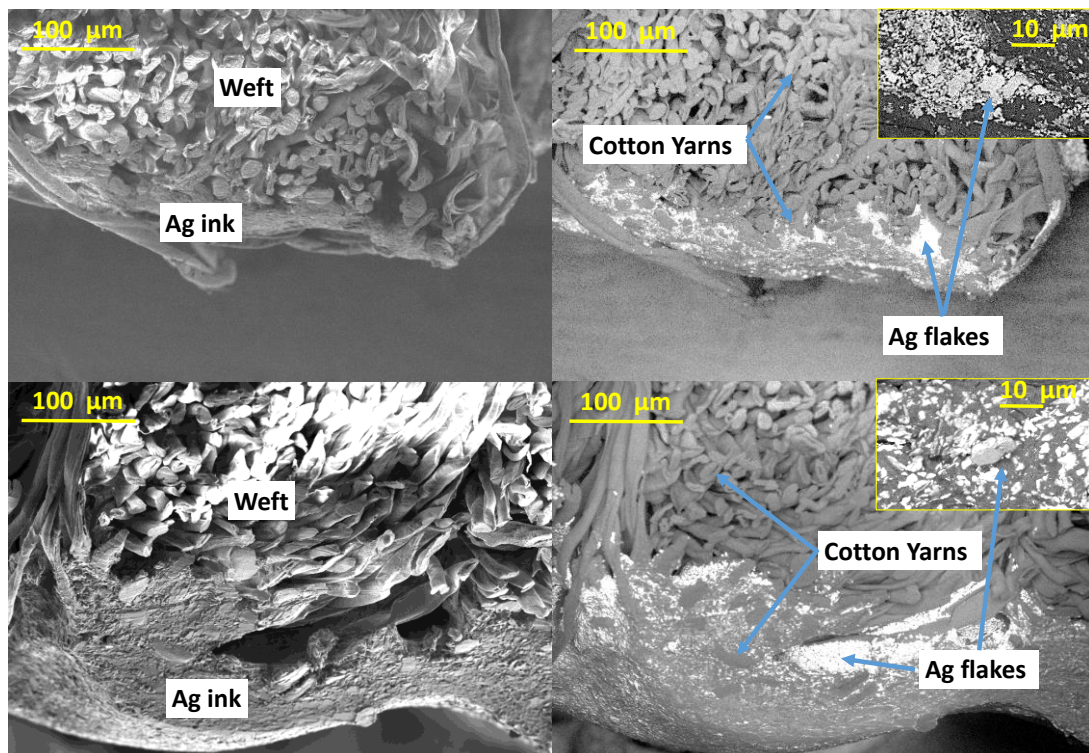


Figure 4. Fabric A printed with DUPONT ink (top) and INKRON ink (bottom). The SE images on the left show a visual characterization of the fabric and ink, and the images on the right show maps of crystalline and textural orientations by EBSD for a determination of the position of the silver particles. In the upper rectangles an enlargement is displayed to visualize the Ag flakes.

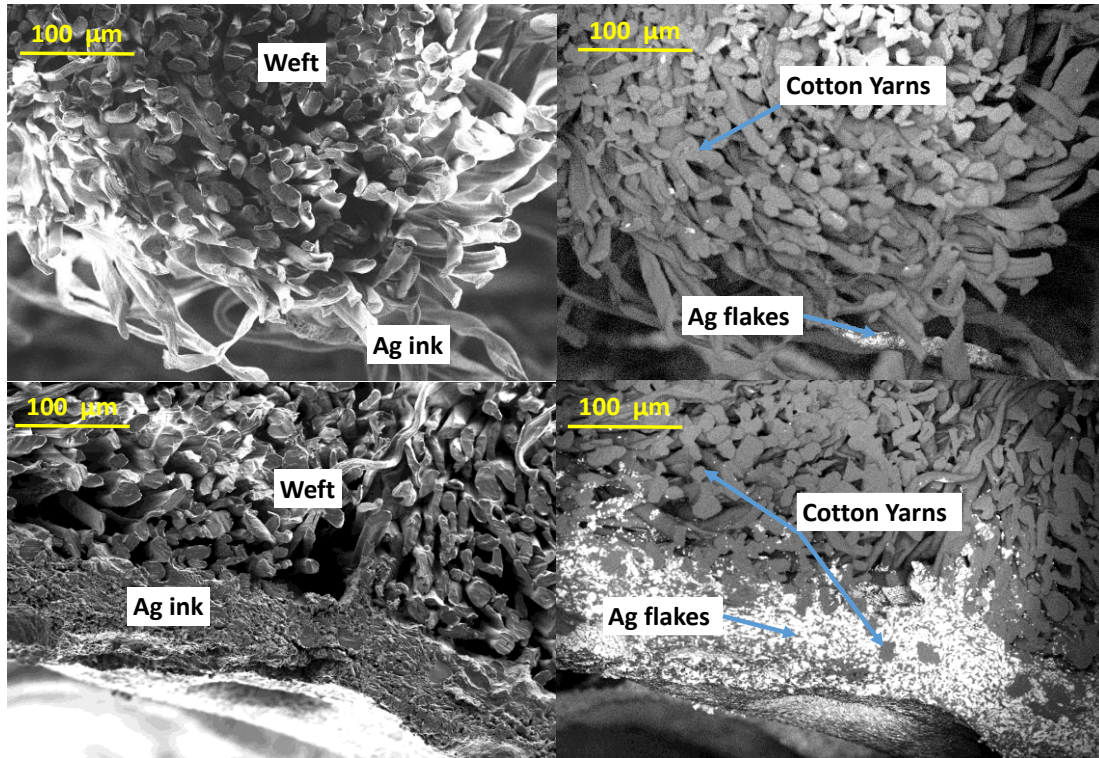


Figure 5. Fabric B printed with DUPONT ink (top) and INKRON ink (bottom). The SE images on the left show a visual characterization of the fabric and ink, and the images on the right show maps of crystalline and textural orientations by EBSD for a determination of the position of the silver particles. In the upper rectangles an enlargement is displayed to visualize the Ag flakes.

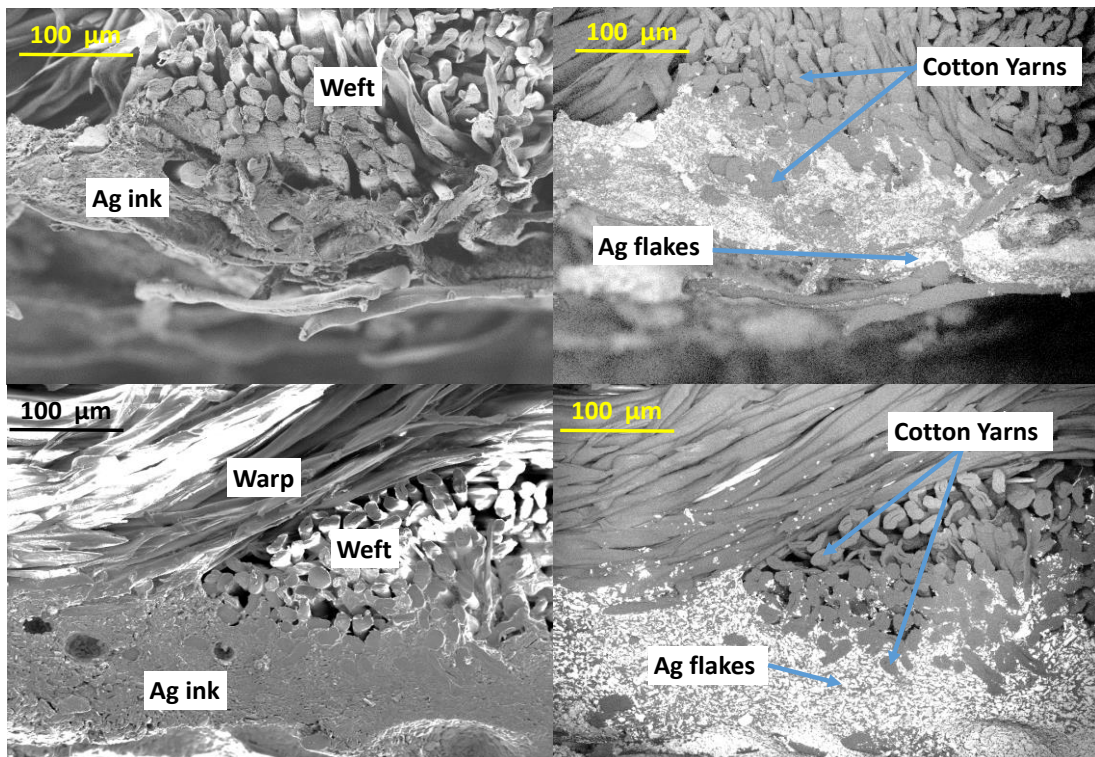


Figure 6. Fabric C printed with DUPONT ink (top) and INKRON ink (bottom). The SE images on the left show a visual characterization of the fabric and ink, and the images on the right show maps of crystalline and textural orientations by EBSD for a determination of the position of the silver particles. In the upper rectangles an enlargement is displayed to visualize the Ag flakes.

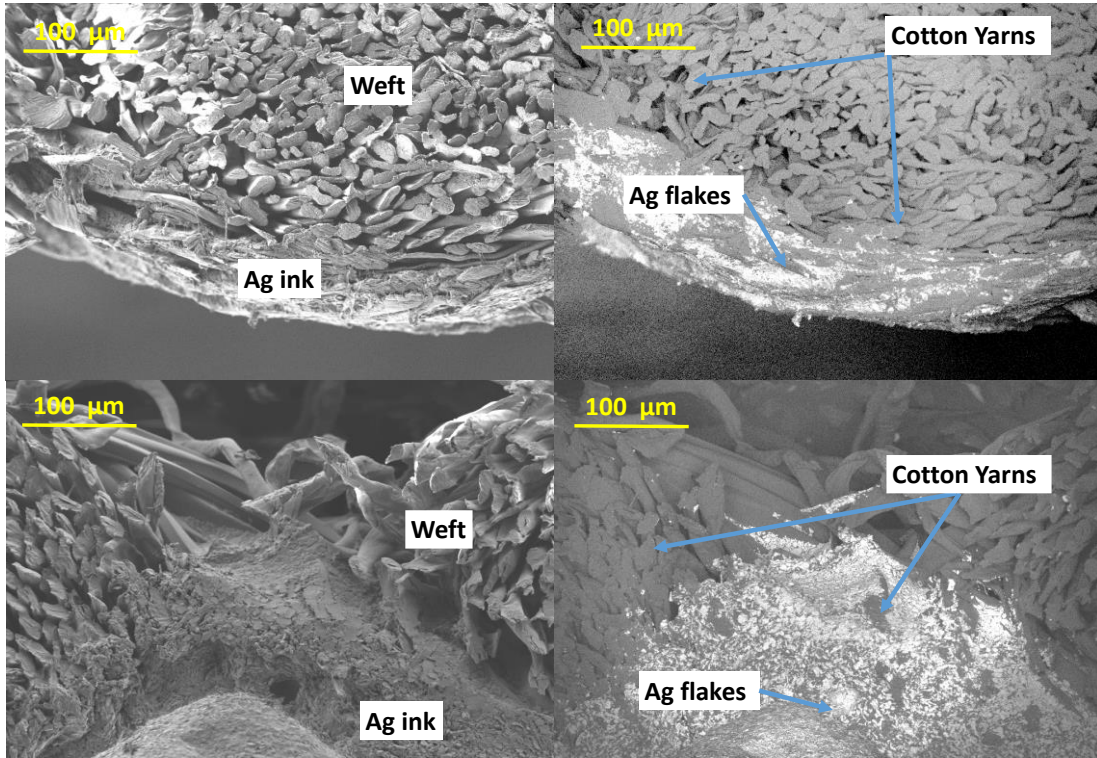


Figure 7. Fabric D printed with DUPONT ink (top) and INKRON ink (bottom). The SE images on the left show a visual characterization of the fabric and ink, and the images on the right show maps of crystalline and textural orientations by EBSD for a determination of the position of the silver particles. In the upper rectangles an enlargement is displayed to visualize the Ag flakes.

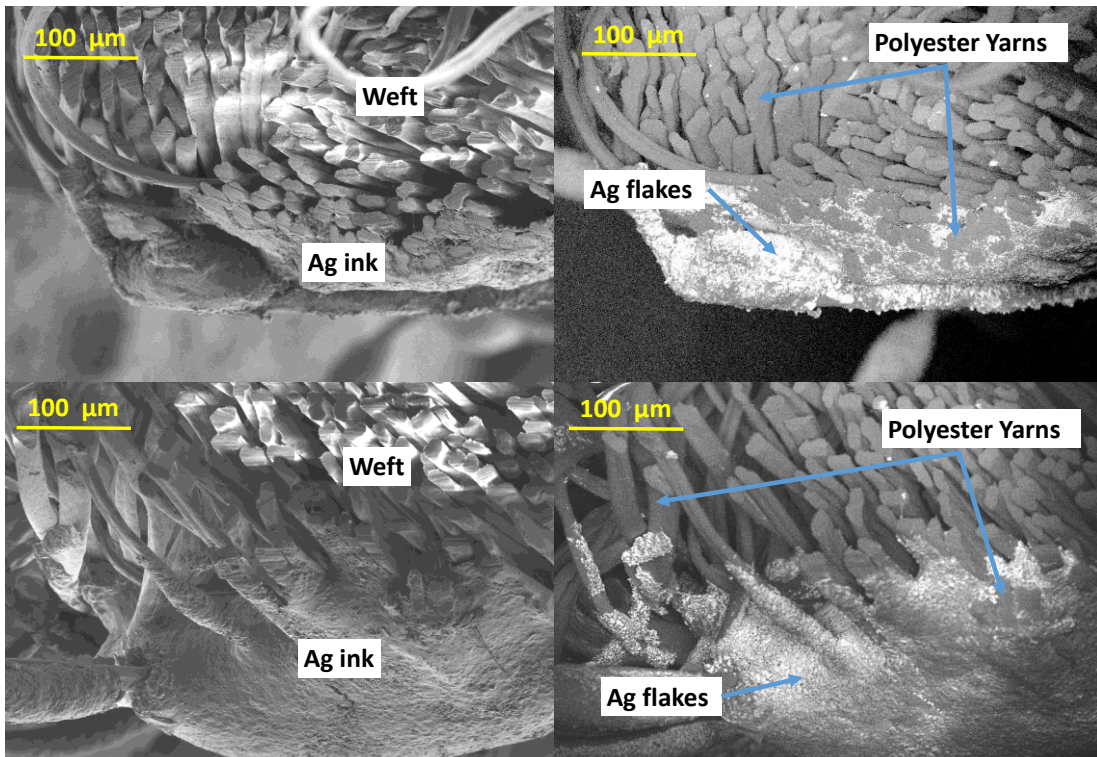


Figure 8. Fabric E printed with DUPONT ink (top) and INKRON ink (bottom). The SE images on the left show a visual characterization of the fabric and ink, and the images on the right show maps of crystalline and textural orientations by EBSD for a determination of the position of the silver particles. In the upper rectangles an enlargement is displayed to visualize the Ag flakes.

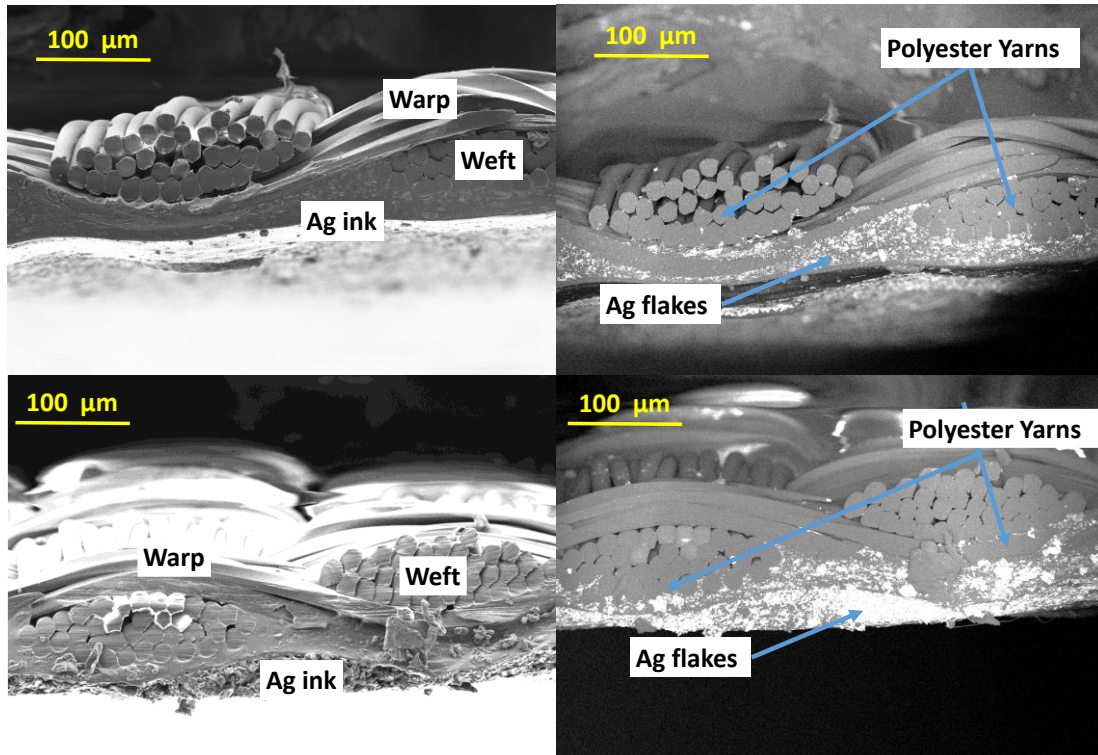


Figure 9. Fabric F printed with DUPONT ink (top) and INKRON ink (bottom). The SE images on the left show a visual characterization of the fabric and ink, and the images on the right show maps of crystalline and textural orientations by EBSD for a determination of the position of the silver particles. In the upper rectangles an enlargement is displayed to visualize the Ag flakes.

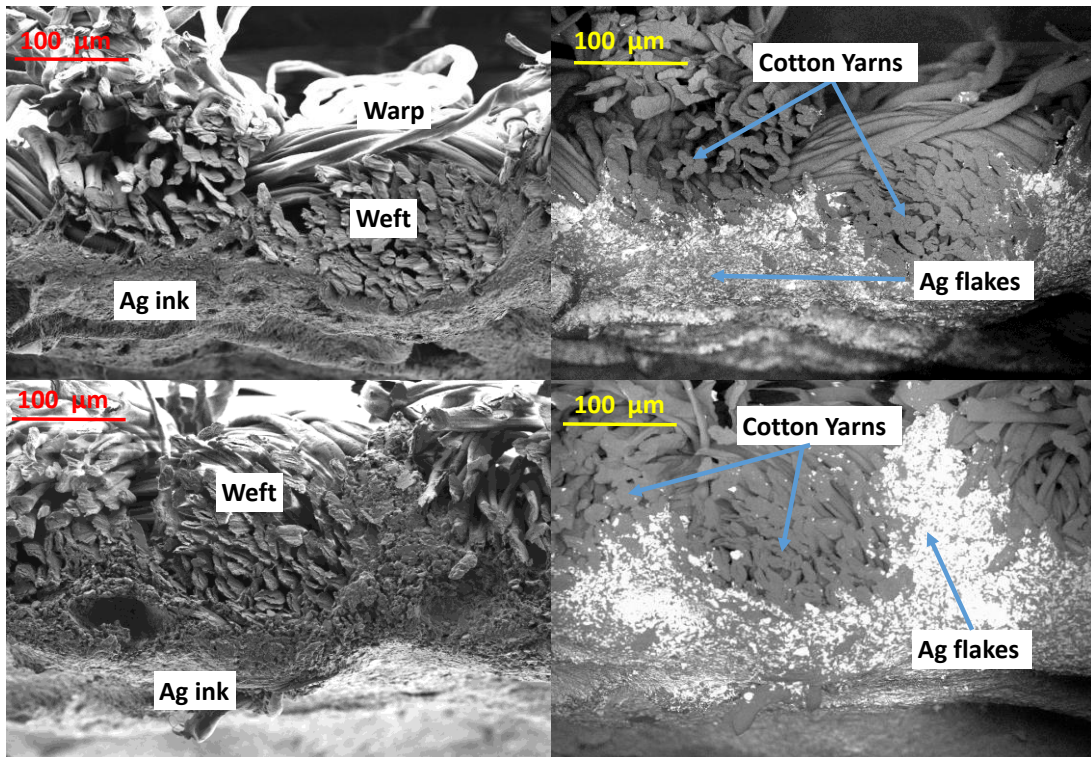


Figure 10. Fabric G printed with DUPONT ink (top) and INKRON ink (bottom). The SE images on the left show a visual characterization of the fabric and ink, and the images on the right show maps of crystalline and textural orientations by EBSD for a determination of the position of the silver particles. In the upper rectangles an enlargement is displayed to visualize the Ag flakes.

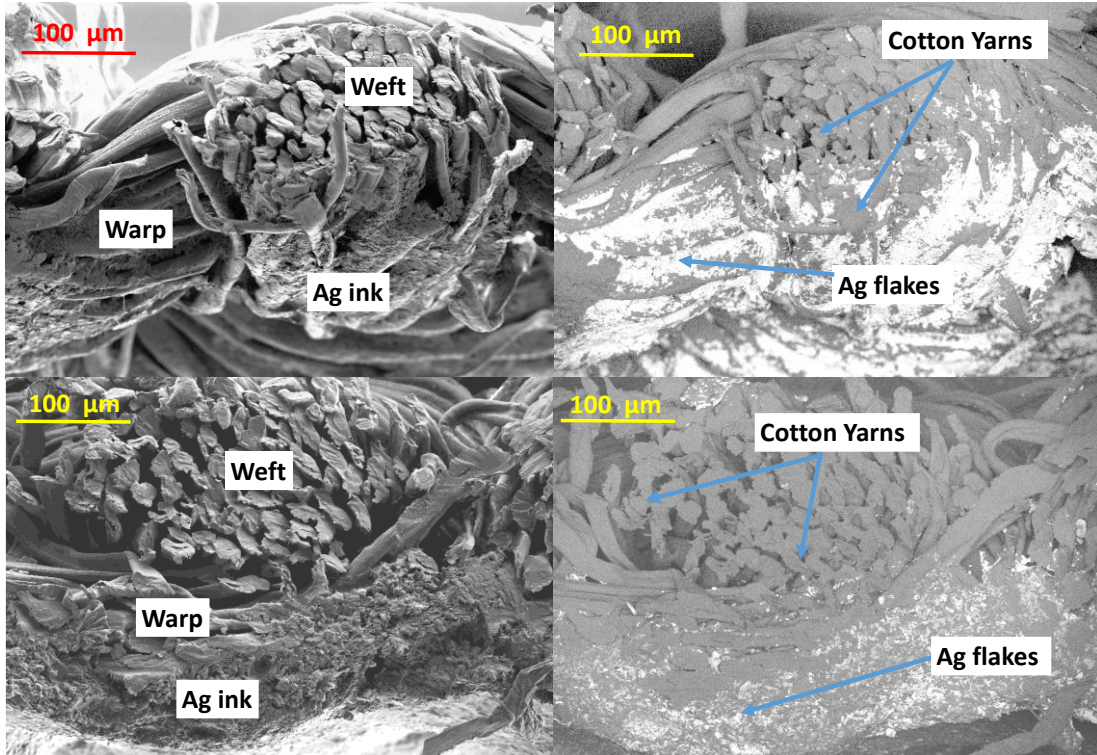


Figure 11. Fabric H printed with DUPONT ink (top) and INKRON ink (bottom). The SE images on the left show a visual characterization of the fabric and ink, and the images on the right show maps of crystalline and textural orientations by EBSD for a determination of the position of the silver particles. In the upper rectangles an enlargement is displayed to visualize the Ag flakes.

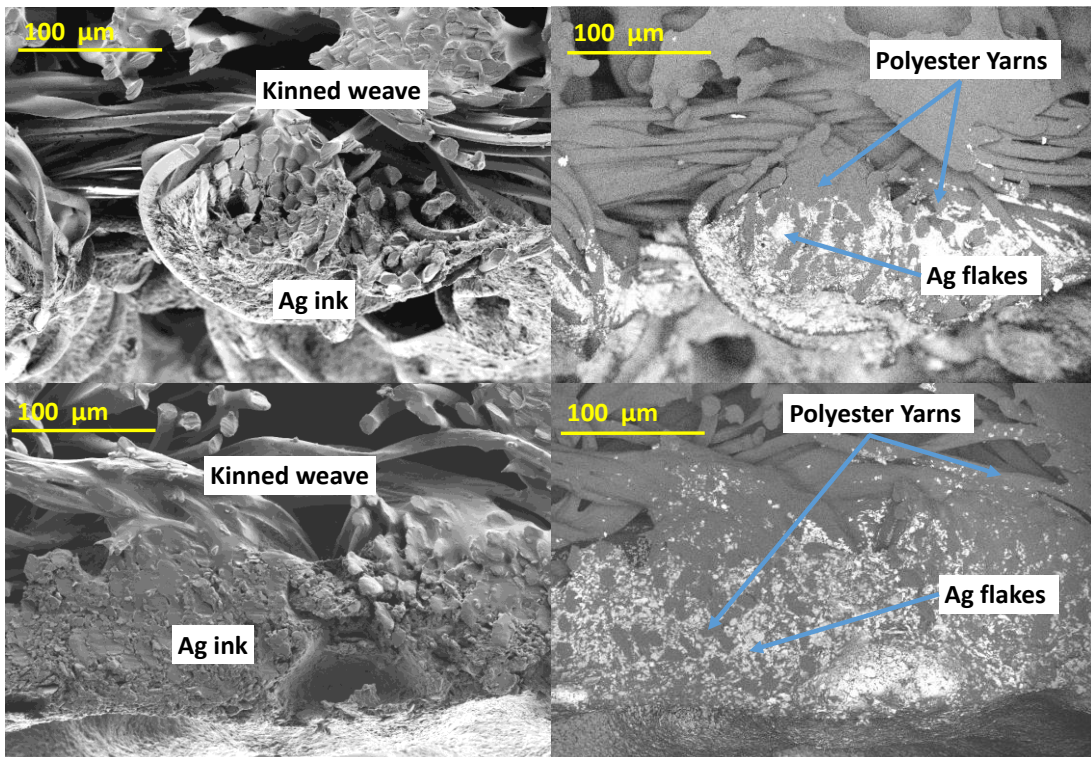


Figure 12. Fabric I printed with DUPONT ink (top) and INKRON ink (bottom). The SE images on the left show a visual characterization of the fabric and ink, and the images on the right show maps of crystalline and textural orientations by EBSD for a determination of the position of the silver particles. In the upper rectangles an enlargement is displayed to visualize the Ag flakes.

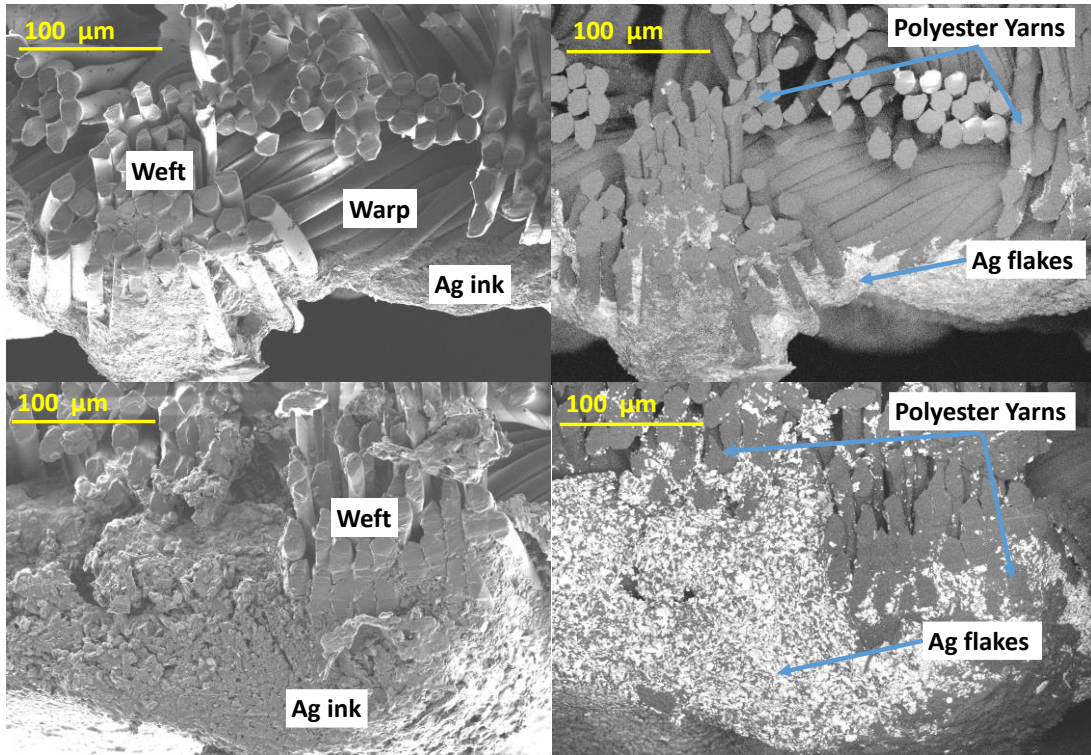


Figure 13. Fabric J printed with DUPONT ink (top) and INKRON ink (bottom). The SE images on the left show a visual characterization of the fabric and ink, and the images on the right show maps of crystalline and textural orientations by EBSD for a determination of the position of the silver particles. In the upper rectangles an enlargement is displayed to visualize the Ag flakes.

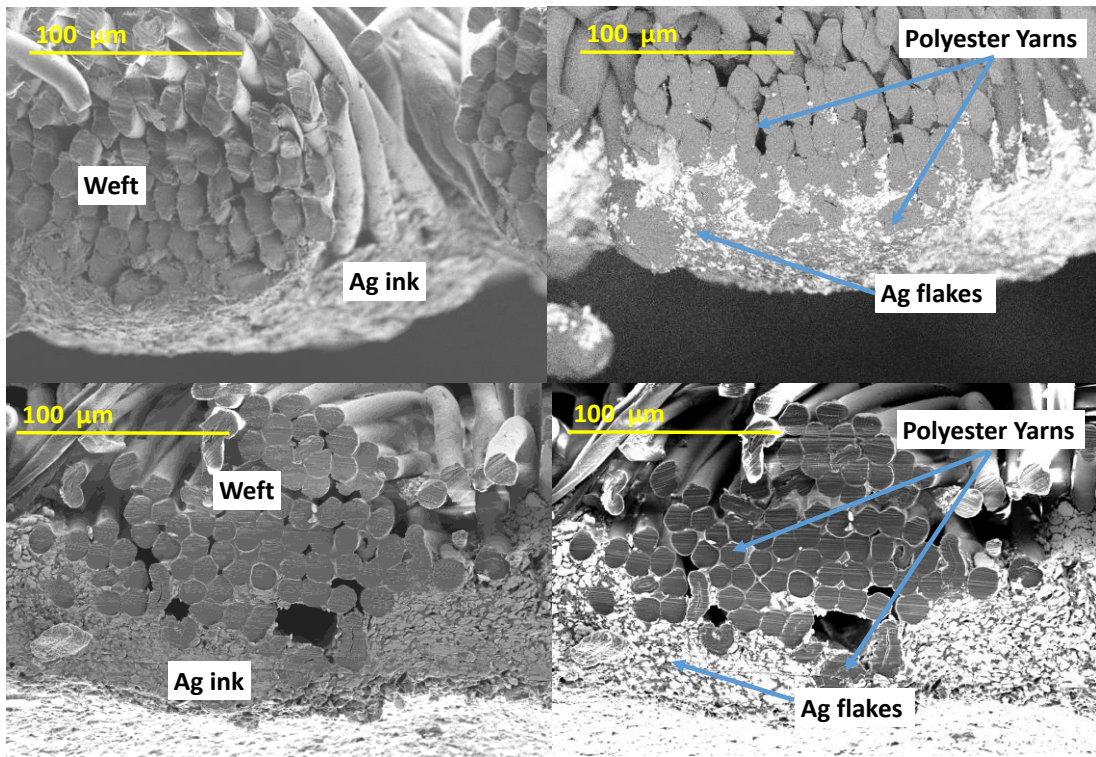


Figure 14. Fabric K printed with DUPONT ink (top) and INKRON ink (bottom). The SE images on the left show a visual characterization of the fabric and ink, and the images on the right show maps of crystalline and textural orientations by EBSD for a determination of the position of the silver particles. In the upper rectangles an enlargement is displayed to visualize the Ag flakes.

The result of the obtained resistance can be observed at a superficial level in Figures 15 and 16. These figures show the shape S4-V with an x8 magnification in function of the type of fabric, type of ink and printing direction, showing in each case the obtained value of resistance.

It can be observed that for the case of the fabrics with higher thickness, lower density and higher diameter of thread, the samples did not show electrical conductivity and the values of resistance obtained were very high (fabrics A, B, C, D and E). In most of these fabrics, it could be observed that the ink did not penetrate in the fabric or the printing was carried out only in the ridges of the fabric with no continuity of the silver through the sample. In the fabrics with the best results, a uniformity in the silver layer was observed, obtaining a higher or lower resistance value according to the quantity of silver that the fabric accepted; visually, it was very clear in fabrics G, H, I, J and K.

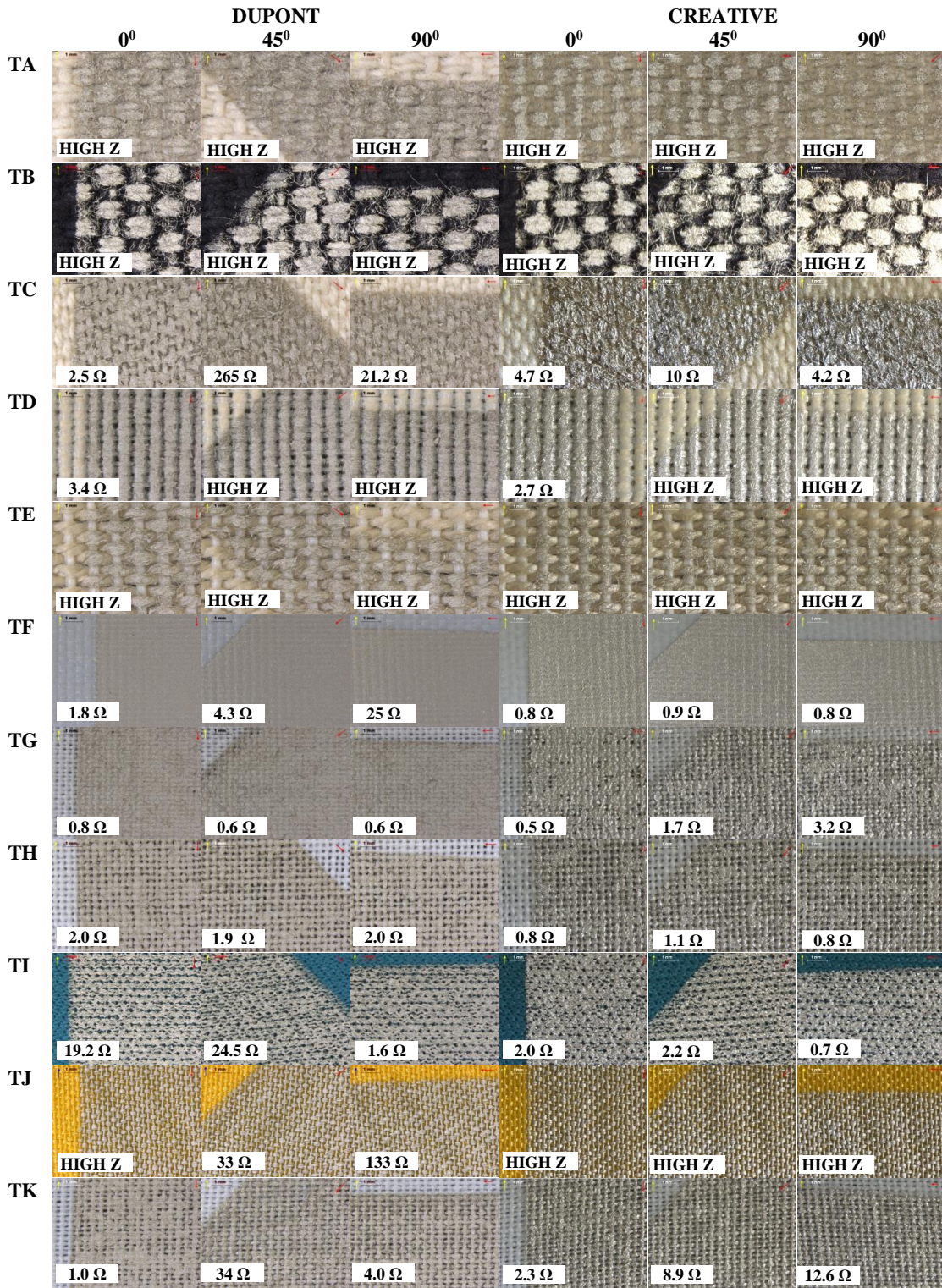


Figure 15. Magnification (x8) of the printings with DUPONT and CREATIVE inks over the different fabrics with different directions of printing. The sample shown is S4-V. In each image, the value of the resistance after the second printing is shown.

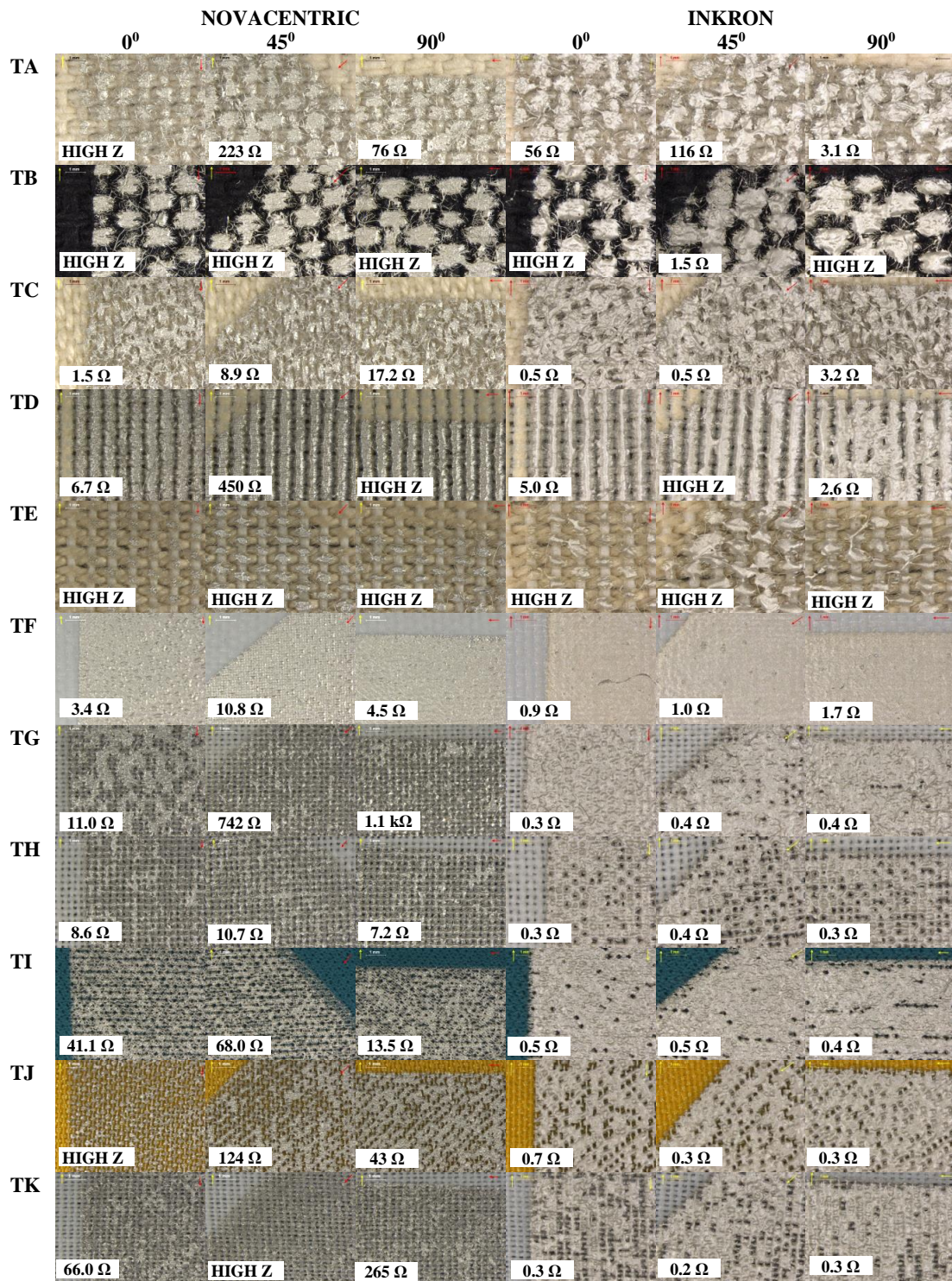


Figure 16. Magnification (x8) of the printings with NOVACENTRIC and INKRON inks over the different fabrics with different directions of printing. The sample shown is S4-V. In each image, the value of the resistance after the second printing is shown.

According to the results shown in Table 9 and Figures 15 and 16, it is possible to study the best printing direction (0°, 45° or 90°). Table 10 shows this study in function of the inks, the shape orientation and the fabrics; in the case of the fabrics, only those fabrics with a good printing result were studied.

Table 10. Optimal printing direction according to the fabric, ink and sample direction. C: circumference, V: vertical, H: horizontal and D: diagonal. 0° same direction as the weft, 90° same direction as the warp and 45° diagonally to both.

| | DUPONT PE873 | | | | CREATIVE 127-48 | | | | NOVACENTRIC HPS-DEV FLX5 | | | | INKRON IPC-603X | | | |
|--------|-----------------|-----|-----|-----|--------------------|-----|-----|-----|-----------------------------|-----|-----|-----|--------------------|-----|-----|-----|
| | C | V | H | D | C | V | H | D | C | V | H | D | C | V | H | D |
| Type F | 0° | 0° | 0° | 0° | 0° | 0° | 0° | 0° | 0° | 0° | 0° | 0° | 45° | 0° | 0° | 0° |
| Type G | 90° | 90° | 90° | 90° | 0° | 0° | 0° | 0° | - | 0° | 0° | 0° | 0° | 0° | 0° | 45° |
| Type H | 0° | 0° | 0° | 0° | 0° | 0° | 0° | 0° | - | 90° | 0° | 0° | 0° | 0° | 0° | 0° |
| Type I | 0° | 90° | 0° | 0° | 0° | 90° | 0° | 45° | - | 90° | 0° | 90° | 45° | 45° | 45° | 45° |
| Type J | - | 0° | 90° | 0° | - | - | - | - | - | 90° | 45° | 45° | 45° | 45° | 90° | 45° |
| Type K | 0° | 0° | 0° | 90° | - | 0° | 90° | 90° | - | 0° | 0° | - | 45° | 45° | 45° | 45° |

To construct Table 10, the smallest value of resistance for each direction was considered. It is worth noting that the choice of the most optimal direction did not imply that the other directions could not be used, but in this case, the results would have a higher resistance value. Hence, from Table 10, it is possible to observe that the most optimal direction was the one that uses the direction of the weft (0°), although some other direction should be considered according to the pattern to be utilized.

Study of the dielectric inks on fabrics

With the aim of improving the printing of the conductive inks on those fabrics with worst results (A, B, C, D, E and K), a printing of a dielectric material was carried out. The used dielectric inks can be found in Table 4. With the printing of an additional ink on the fabric it was expected to penetrate covering the bundle of fibers that composed the thread of the weft with the warp, improving the roughness. In this way, the subsequent conductive ink printing was expected to have better conductivity results. In the case of fabrics A and B, since they were very similar, the study was only performed on fabric A. The procedure of this phase has been detailed in the Experimental Procedure point.

Figure 17 shows the result of the printing of the three dielectric inks on the fabrics. In the case of fabrics A, C, D and E, the inks were embedded inside of the fabric, thus there still existed roughness, and a good planarity was not obtained. In the fabric K, good results were obtained with any of the three inks. When comparing the roughness values of the fabrics without dielectric (Table 8) with the values with dielectric (Table 11), it can be observed that only the EMS DI-7542 ink improved the roughness in all the fabrics. With the other two inks, the indices of roughness were maintained or even worsened.

Table 11. Parameters of fabrics' roughness with dielectrics.

| | Ra (µm) | Rq (µm) | Rz (µm) |
|-------------------------|----------------|----------------|----------------|
| Type A+CREATIVE 127-48D | 40.52 | 49.24 | 229.37 |
| Type A+EMS DI-7542 | 31.15 | 36.47 | 181.12 |
| Type A+INKRON IPD-670 | 30.61 | 37.18 | 178.41 |
| Type C+CREATIVE 127-48D | 29.40 | 34.86 | 171.05 |
| Type C+EMS DI-7542 | 23.36 | 28.46 | 146.94 |
| Type C+INKRON IPD-670 | 28.01 | 34.43 | 197.13 |
| Type D+CREATIVE 127-48D | 37.06 | 46.10 | 243.00 |
| Type D+EMS DI-7542 | 27.56 | 34.54 | 185.76 |
| Type D+INKRON IPD-670 | 28.53 | 29.83 | 180.57 |
| Type E+CREATIVE 127-48D | 56.11 | 67.76 | 298.67 |
| Type E+EMS DI-7542 | 38.85 | 47.61 | 251.49 |
| Type E+INKRON IPD-670 | 47.02 | 59.58 | 344.08 |
| Type K+CREATIVE 127-48D | 17.77 | 22.92 | 133.15 |
| Type K+EMS DI-7542 | 11.54 | 14.93 | 96.53 |
| Type K+INKRON IPD-670 | 18.12 | 26.95 | 168.48 |

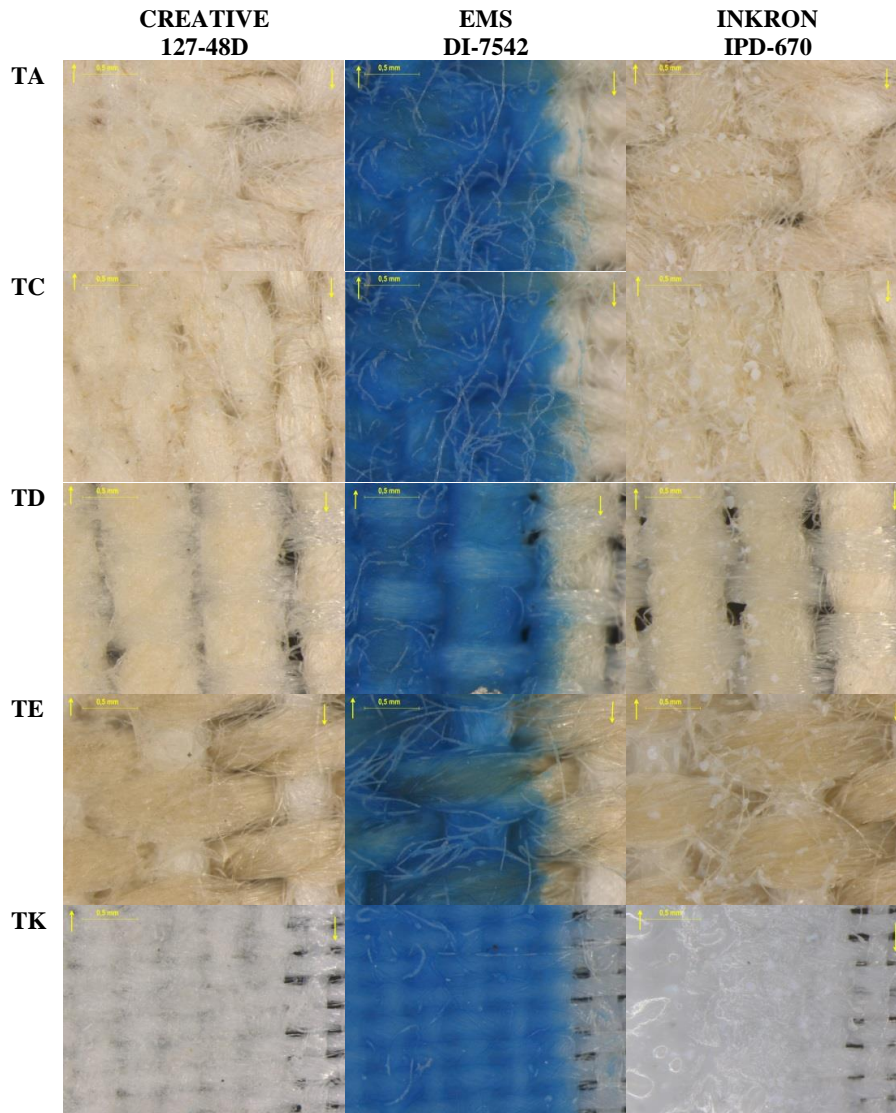


Figure 17. Magnification (x25) of the printings with dielectric inks on the different fabrics. The printing was carried out according to the weft direction (0°).

After the printing of the dielectric inks, a printing of the conductive ink was made to study the values of resistance obtained. Table 12 shows the value of the resistance of the more significant samples (in this case, the ones with the highest size) in function of the type of fabric and shape orientation. According to the results reflected in Table 10, it was decided to print in the weft direction (0°). Moreover, according to the results shown in Tables 7 and 9, it was decided to use the ink with the worst results, i.e. CREATIVE, with the aim of assessing whether the printing improved. The results are shown in Figure 18 and Table 12, concluding that the conductive ink printing on these fabrics did not improve after using the dielectric inks. Only in the case of the fabric K, a good printing was obtained. For this fabric, the lowest resistance values were obtained when printing directly on the fabric, although the best percentage of samples showing conductivity were obtained in the case of the addition of the dielectric layer with dielectrics EMS DI-7542 and INKRON IPD-670.

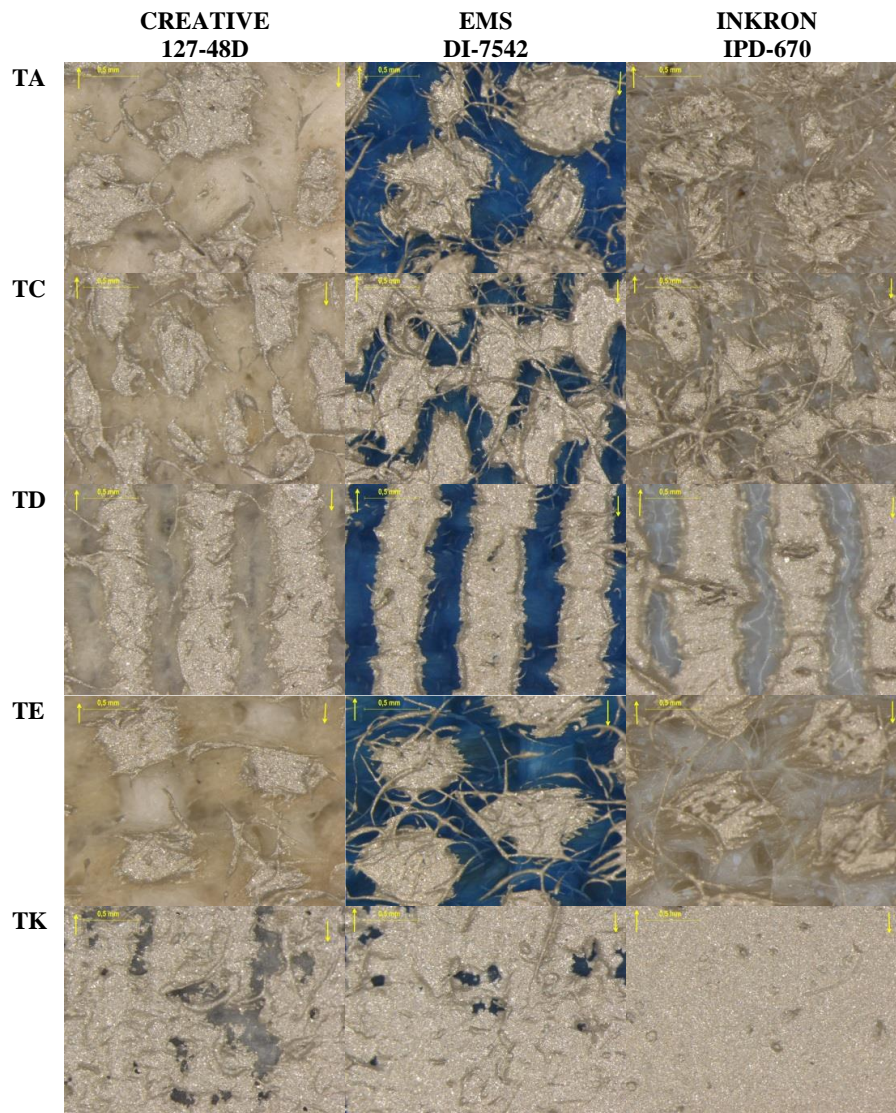


Figure 18. Magnification (x25) of the printings with the conductive inks on the different dielectrics. The printing was carried out according to the weave direction (0°). Ink CREATIVE 127-48.

Table 12. Resistance value (Ω) of the most significant samples (larger size) depending on the fabrics and dielectrics and sample orientation for CREATIVE 127-48 Silver ink. Direction of the printing is 0° (same direction as the weft). The measurement is made after the second printing.

| | | Without Dielectric | CREATIVE 127-48D | EMS DI-7542 | INKRON IPD-670 |
|--------|-------|-----------------------|---------------------|----------------|-------------------|
| Type A | S3-C | - | - | - | - |
| | S4-V | - | - | - | - |
| | S5-H | - | - | - | - |
| | S13-D | - | - | - | - |
| Type C | S3-C | - | - | - | - |
| | S4-V | 4.7 | 299 | - | - |
| | S5-H | 3.2 | 85 | - | - |
| | S13-D | 4.3 | 33 | - | 50 |
| Type D | S3-C | - | - | - | - |
| | S4-V | 2.7 | 60 | 150 | 14 |
| | S5-H | - | - | - | - |
| | S13-D | - | - | - | 10 |
| Type E | S3-C | - | - | - | - |
| | S4-V | - | - | - | - |
| | S5-H | - | - | - | - |
| | S13-D | - | - | - | - |
| Type K | S3-C | - | - | 68 | 27 |
| | S4-V | 2.3 | 9.4 | 14 | 7 |
| | S5-H | 8.5 | 2.4 | 2.6 | 8.8 |
| | S13-D | 1.1 | 1.8 | 6 | 6.4 |

Study of the polyurethane films on fabrics

As an alternative to the dielectrics to improve the printing of the conductive ink, it was decided to use polyurethane films (Table 5) due to their dielectric characteristics and easiness to be stuck to the fabrics. After heat sealing the polyurethanes, the printing of the conductive ink was made with the results shown in Table 13. The obtained results were excellent in all the cases, with resistance values very close to the reference measurements on the PET substrate (Table 6) and with a percentage of samples with conductivity of 100%. Thus, the use of polyurethane films allowed to carry out printings of conductive inks on those fabrics where the direct printing was not viable.

Since the mechanical behaviour of the films is different to the one corresponding to the fabrics, a parallel study of enlargement of these films was carried out. The study allowed to assess the behaviour in terms of enlargement of the conductive inks as well. The study was carried out for the most stretchable ink (INKRON) and for one of the non-stretchable (CREATIVE). The process has been detailed in the Experimental Procedure point. The studied fabrics admitted a maximum enlargement up to 10% (most restrictive fabric) or 350% (less restrictive fabric) as shown in Table 14. Since the most restrictive value of enlargement is 10% in the fabrics, the study of the polyurethanes was carried out up to a maximum value of 10%.

Figure 19 shows the percentual increment of the value of the resistance in function of the elongation of the sample for the four films of polyurethane and for the CREATIVE and INKRON inks. The non-stretchable ink (CREATIVE) suffered a high variation in the value of the resistance of the samples, achieving a 650% of increment of resistance at a 10% of elongation against the 250% obtained with the INKRON ink. The type of polyurethane film influenced the final result as well, observing that with DELSTAR EU94, lower resistance increments were obtained, increasing progressively with the films EU50, INSPIRE 2370 and UAF-455. Considering a maximum elongation of 10% of a square surface in the two axis produces that the area only increments 2%. The capacity would be affected by the increment of the size of the area of the conductive plates during the elongation; from the values of real capacity obtained (Table 19), it is possible to deduce that in the worst case, a variation of the capacity of 2% is admitted to remain in the range up to 60 pF, since the relation is linear. For elongation values lower than 2%, the films EU50, INSPIRE 2370 and UAF455 behaved in a similar way, obtaining the best results with the EU94DS film and the INKRON ink. In the 2% range of elongation, the inks suffered an increment of the value of the resistance of the pattern of up to 50%. Although these values can be significative, they should not have a big influence in the value of the capacity of the sensor since this does not depend on the conductivity value of the conductive plates of the capacitor. Although the UAF-445 film did not present the best results according to conductivity it was decided to use this film since it was the one that showed the best adherence over all the studied fabrics. It was selected this film as a balanced

solution between conductivity performance and good adhesion to the most of the textiles considering the selected heating attachment solution.

Table 13. Resistance value (Ω) of the most significant samples (larger size) depending on the fabrics and polyurethanes and sample orientation for CREATIVE 127-48 Silver ink. The measurement is made after the second printing.

| | | DELSTAR EU50 | DELSTAR EU94DS | INSPIRE 2370 | ADHESIVE FIMS UAF-445 |
|--------|-------|-----------------|-------------------|-----------------|-----------------------------|
| Type A | S3-C | 35.8 | 23.5 | 21.7 | 18.7 |
| | S4-V | 5.3 | 3.1 | 2.7 | 2.9 |
| | S5-H | 3.7 | 1.8 | 1.5 | 2.3 |
| | S13-D | 1.3 | 1.7 | 1.3 | 1.3 |
| Type C | S3-C | 25.4 | 30.8 | 11.3 | 20.9 |
| | S4-V | 2.9 | 3.9 | 2.2 | 5.6 |
| | S5-H | 1.7 | 2.8 | 1.0 | 3.0 |
| | S13-D | 1.7 | 2.1 | 1.1 | 2.8 |
| Type D | S3-C | 16.2 | 24.2 | 15.0 | 26.0 |
| | S4-V | 2.0 | 4.3 | 2.2 | 5.2 |
| | S5-H | 1.8 | 2.3 | 1.5 | 3.9 |
| | S13-D | 1.0 | 2.4 | 1.7 | 3.4 |
| Type E | S3-C | 16.9 | 12.8 | 10.7 | 19.1 |
| | S4-V | 2.5 | 2.4 | 2.5 | 4.5 |
| | S5-H | 1.5 | 1.3 | 1.2 | 2.1 |
| | S13-D | 1.0 | 1.4 | 1.8 | 1.8 |
| Type K | S3-C | 21.3 | 20.4 | 15.4 | 27.0 |
| | S4-V | 3.9 | 2.9 | 3.0 | 5.1 |
| | S5-H | 2.8 | 3.5 | 2.0 | 2.8 |
| | S13-D | 2.1 | 1.5 | 1.6 | 2.4 |

Table 14. Maximum enlargement in the warp and weft directions [%]

| | Warp | Weft |
|--------|------|------|
| Type A | 27 | 19 |
| Type B | 10 | 23 |
| Type C | 16 | 15 |
| Type D | 53 | 16 |
| Type E | 40 | 24 |
| Type F | 31 | 34 |
| Type G | 18 | 18 |
| Type H | 10 | 18 |
| Type I | 350 | 110 |
| Type J | 61 | 67 |
| Type K | 26 | 35 |

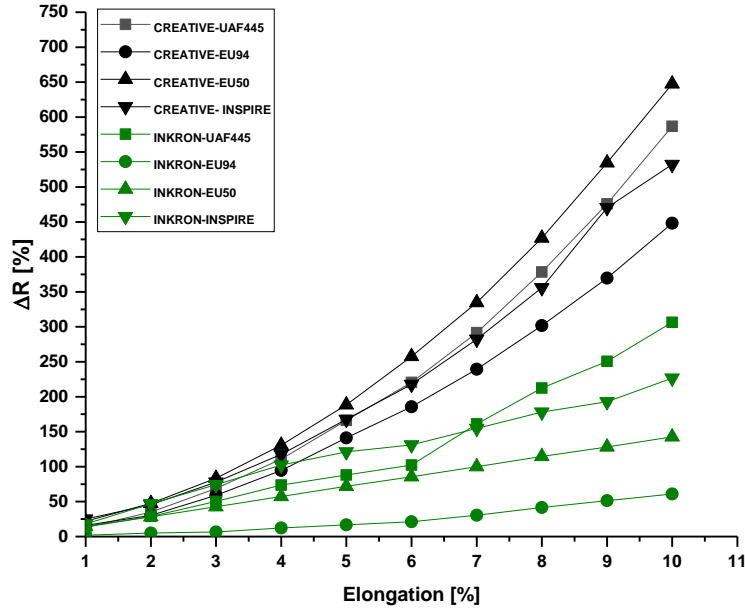


Figure 19. Percentual increment of the value of resistance in function of the elongation of the sample for the four films of polyurethane and for the inks CREATIVE and INKRON.

Study of the expected capacitance of a capacitive sensor on fabrics

A study of the relative permittivities (ϵ_r) of the different materials used in this work was carried out. Table 15 shows the ϵ_r of the fabrics. Table 16 shows the ϵ_r of the fabrics that needed a dielectric layer on their surface (A, B, C, D, E and K) for each one of the dielectric inks used. Regarding the polyurethane films, the evaluation was carried out in two ways, on the one hand, the film alone with no fabric, and on the other hand, the film attached to the fabric. Table 17 shows the ϵ_r of the fabrics with polyurethane films in one and in both sides of the fabric. Lastly, Table 18 shows the ϵ_r of all the fabrics with a film of UAF-445 polyurethane chosen to make the flat capacitor prototypes.

Table 15. Relative permittivity of fabrics ϵ_r @ 100 kHz

| Fabric | Relative Permittivity |
|--------|-----------------------|
| Type A | 2.64 |
| Type B | 2.65 |
| Type C | 2.58 |
| Type D | 1.93 |
| Type E | 1.37 |
| Type F | 2.37 |
| Type G | 1.83 |
| Type H | 2.60 |
| Type I | 1.84 |
| Type J | 1.49 |
| Type K | 1.73 |

Table 16. Relative permittivity of the dielectric inks on fabrics ϵ_r @100 kHz

| | CREATIVE 127-48D | EMS DI-7542 | INKRON IPD-670 |
|---------------|---------------------|----------------|-------------------|
| PET substrate | 1.72 | 5.68 | 4.20 |
| Type A | 2.04 | 2.98 | 3.68 |
| Type C | 5.38 | 2.98 | 3.37 |
| Type D | 3.91 | 2.32 | 3.07 |
| Type E | 2.83 | 1.96 | 2.95 |
| Type K | 1.33 | 1.73 | 2.22 |

Table 17. Relative permittivity of the polyurethanes on fabrics ϵ_r @100 kHz

| | DELSTAR EU50 | DELSTAR EU94DS | INSPIRE 2370 | ADHESIVE FIMS UAF-445 |
|---------------------|-----------------|-------------------|-----------------|-----------------------------|
| Film with no fabric | 1.30 | 1.46 | 1.37 | 1.86 |
| Type A | 1 layer | 2.33 | 2.52 | 2.20 |
| | 2 layers | 2.33 | 3.30 | 2.76 |
| Type C | 1 layer | 2.20 | 2.45 | 2.07 |
| | 2 layers | 2.34 | 2.96 | 2.53 |
| Type D | 1 layer | 2.05 | 2.08 | 1.81 |
| | 2 layers | 2.21 | 2.91 | 1.98 |
| Type E | 1 layer | 1.79 | 1.86 | 1.73 |
| | 2 layers | 1.67 | 2.36 | 1.65 |
| Type K | 1 layer | 1.80 | 1.98 | 1.55 |
| | 2 layers | 2.97 | 2.89 | 1.96 |

Table 18. Relative permittivity of fabrics with UAF445 ϵ_r @100 kHz

| Fabric | Relative Permittivity | |
|--------|-----------------------|----------|
| | 1 layer | 2 layers |
| Type A | 2.87 | 2.88 |
| Type B | 2.02 | 2.24 |
| Type C | 2.57 | 2.79 |
| Type D | 2.36 | 2.64 |
| Type E | 2.05 | 2.18 |
| Type F | 2.32 | 3.07 |
| Type G | 2.59 | 3.22 |
| Type H | 3.73 | 3.76 |
| Type I | 2.02 | 2.47 |
| Type J | 1.6 | 2.4 |
| Type K | 2.23 | 2.96 |

With these values of relative permittivity and the dielectric thickness obtained (fabric, fabric + dielectric ink and fabric + polyurethane), an analysis of the value of the expected capacity for a flat capacitor was performed.

Figure 20 shows the values of the expected capacity using only the fabrics. To achieve low values of capacity, high thicknesses of layer and low relative permittivities are required. Figure 20 shows that fabric E obtained capacities of approximately 10 pF, but it was a fabric that did not allow to print a conductive ink directly. Fabrics A, B, C and D had high values of thickness that compensated their high values of relative permittivity, obtaining capacities between 30 and 40 pF. In any case, the printing of conductive ink directly over them was not very feasible. Fabrics F, G and H, that best allowed the direct printing, had a very low value of thickness and a high value of dielectric permittivity, therefore achieving very high values of capacity (> 90 pF). Lastly, fabrics I, J and K had balanced values of thickness and permittivity, obtaining values of capacity between 40 and 60 pF as well.

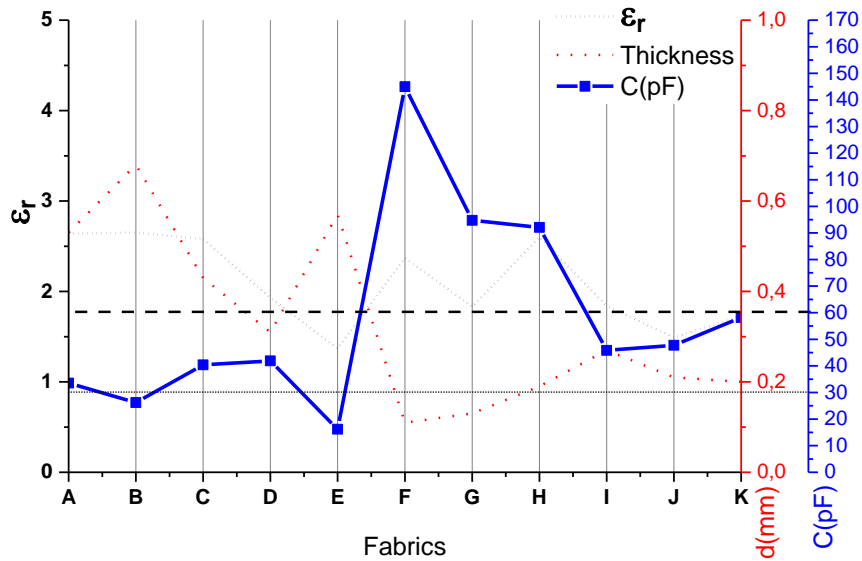


Figure 20. Expected value of the capacity in function of the fabrics.

Figure 21 shows the expected value of the most problematic fabrics (A, C, D, E and K) with the dielectric inks. Fabric B values have been omitted for being very similar to fabric A values. In addition, when adding the dielectric layer, a higher total thickness of dielectric was obtained and, therefore, the capacities could decrement, as long as the total relative permittivity of the fabric and the dielectric did not increment excessively. Looking at this variation with fabric A, with an expected capacity of 38 pF (Figure 20), a variation oscillating between 19 and 35 pF was obtained, depending on the dielectric ink applied (Figure 21). With fabric C, with a capacity of 60 pF, the variation was between 34 and 62 pF. In fabric D, with a capacity of 40 pF, the corresponding variation was between 39 and 67 pF. Fabric E, with a capacity of 13 pF, suffered a variation between 20 and 31 pF. Lastly, for fabric K, with 63 pF of capacity, the obtained variation was between 45 and 76 pF. The variation was not due to the same dielectric, but to the influence of the dielectric on the total relative permittivity and not on the total thickness that did not seem to have much variation. For fabrics A and K, the best dielectric is CREATIVE 127-48D and for fabrics C, D and E, the best one is EMS DI-7542. The permittivity of fabrics A and K was reduced with CREATIVE 127-48D but was incremented with the rest. On the other hand, for fabrics C, D and E, the permittivity was incremented with all the dielectrics, but the increment was lower with EMS DI-7542. The variations of the permittivity could be related to the quantity of air between the fabric and the dielectric after the printing and to the irregularity of the dielectric ink through the fabric.

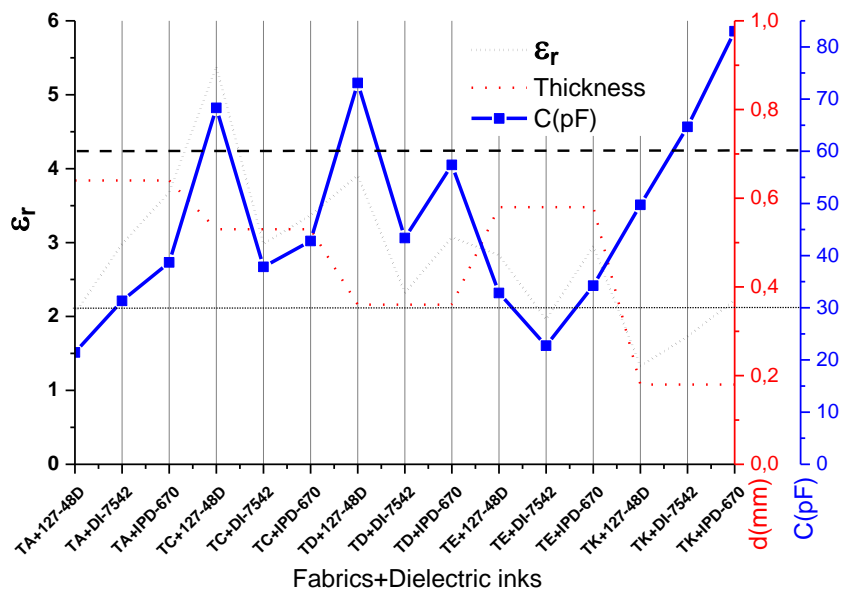


Figure 21. Expected value of the capacity in function of the fabrics with dielectric ink

Figure 22 shows the expected value for the same problematic fabrics (A, C, D, E and K) and the polyurethane film. Fabrics A, C and D had low values of thickness and high values of relative permittivity, obtaining capacities between 20 and 40 pF. Fabric E obtained capacities below 25 pF. The results are quite similar for each fabric using the different polyurethanes. Lastly, fabric K had a very low value of thickness and a relative permittivity valuer between 1.5 and 2, therefore achieving very high values of capacity (>70 pF), except for Inspire polyurethane that obtains 55 pF, under the threshold of 60 pF.

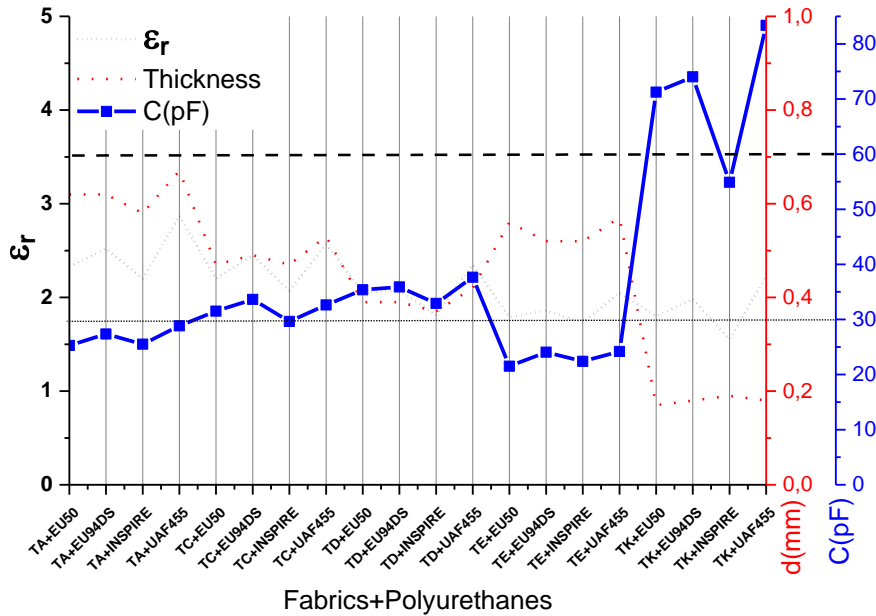


Figure 22. Expected value of the capacity in function of the fabrics with a polyurethane film in only one side of the fabric.

As the polyurethanes has similar results on the same fabric, one of them was selected for further test. Focusing only on one polyurethane film, UAF-455, it was possible to determine the estimated value of the capacity when the polyurethane is applied in only one side (Figure 23) and in both sides of the fabric (Figure 24). In the first case, fabrics A, B and E allowed to obtain capacities lower than 30 pF and fabrics C, D, I, J and K lower than 60 pF. Fabrics F, G and H exceeded the limit of 60 pF. In the case of two layers de polyurethane, the capacity was improved in all the fabrics, except in fabric F, that was rejected since it exceeded 60 pF.

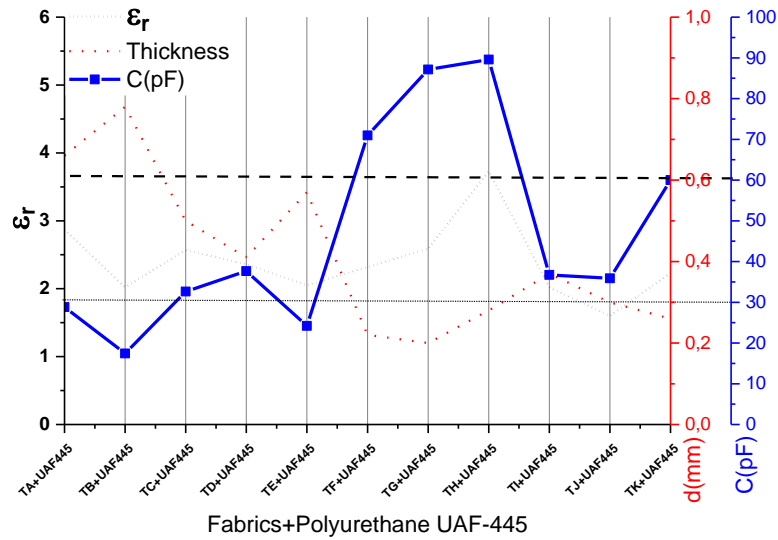


Figure 23. Expected value of the capacity in function of the fabrics with a polyurethane film EUF-455 in only one side of the fabric.

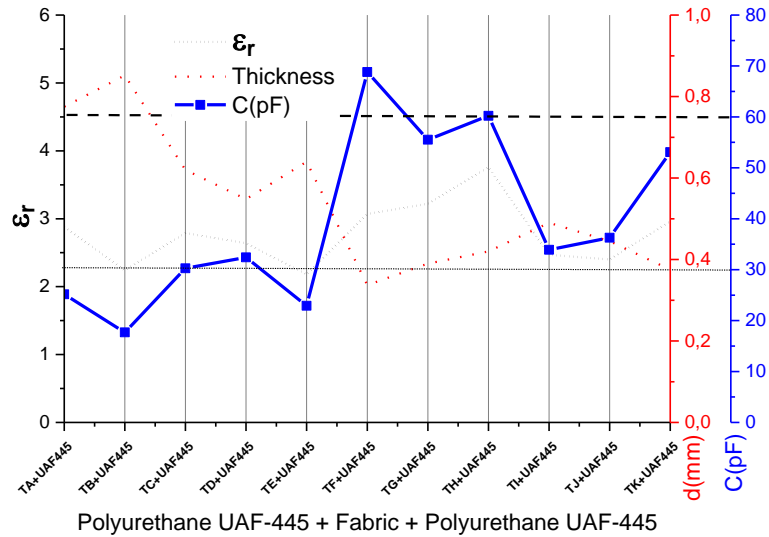


Figure 24. Expected value of the capacity in function of the fabrics with a polyurethane film EUF-455 in both sides of the fabric.

Study of the real capacitance of a capacitive sensor on fabrics

To finish the experimental part, flat capacitors were printed using all the fabrics. The conductive inks were printed directly on the fabrics that allowed it. To avoid short circuits between the plaques of the capacitor, films of polyurethane were used on one of the sides on those fabrics where the conductive ink was printed directly on one of the layers (Figure 25.b). For the fabrics that did not allowed to print the conductive inks, two films of polyurethane (one in each side) were used (Figure 25.a).

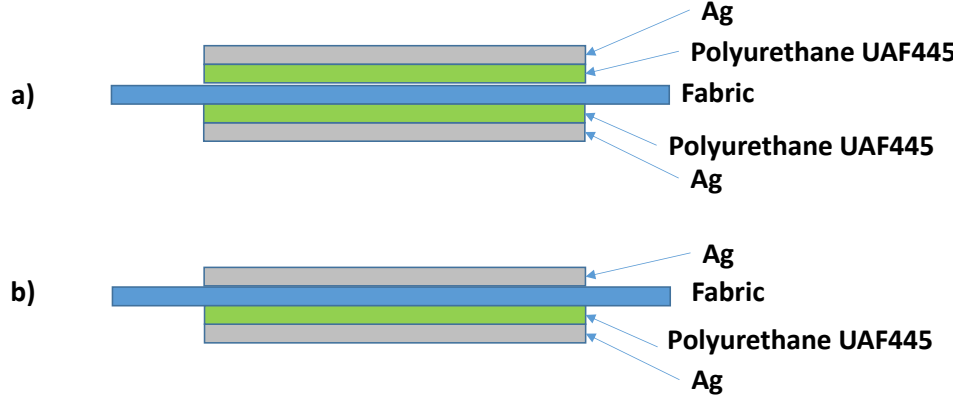


Figure 25. Structures used for the capacitor: a) Polyurethane on both sides (named Ca) and b) Polyurethane in only one side (named Cb).

The real value obtained when measuring each one of the capacitors was compared with the theoretical nominal value (C_n) and with the capacity value with the Edge effect (C_{edge}). This latter value considers the effect of the field lines in the edges of the capacitor and can be calculated according to Equations 4 and 5.

$$C_{edge} = \frac{0.0885 \cdot \epsilon_r \cdot (L + \Delta f) \cdot (w + \Delta f)}{t} \quad (4)$$

$$\Delta f = t + \frac{0.0885 \cdot t \cdot 10 \cdot \ln((L + w) + 1)}{\pi} \quad (5)$$

where C_{edge} is the value of the capacity in pF, L is the length in cm, w is the width in cm, t is the thickness in cm and ϵ_r is the relative permittivity.

Table 19 shows the values of the theoretical capacities and the real value measured with an LCR meter. The values for fabrics A, B, C, D and E with polyurethane in only one side have been omitted because of the difficulty to obtain continuity on the side without polyurethane. Figure 26 shows graphically the results of Table 19. In general, the theoretical results are validated by the real ones, except for the fabric type F, H and I with the type Cb capacitor (polyurethane on one side). The reduction of the thickness value of the fabrics against theoretical thickness value can be explained due to the compaction during the heat sealing process to attach the polyurethane.

Table 19. Values of the theoretical nominal capacity (C_n), with Edge effect (C_{edge}) and real values (C_{real}) for the fabrics with polyurethanes on both sides (Ca) and on one side (Cb).

| | Ca (pF) | | | Cb (pF) | | |
|--------|---------|------------|-------------|---------|------------|--------------|
| | C_n | C_{edge} | C_{real} | C_n | C_{edge} | C_{real} |
| Type A | 25.16 | 28.73 | 32.13±10.64 | - | - | - |
| Type B | 17.69 | 20.48 | 29.46±10.68 | - | - | - |
| Type C | 30.27 | 33.72 | 38.45±10.76 | - | - | - |
| Type D | 32.42 | 35.68 | 37.44±10.74 | - | - | - |
| Type E | 22.91 | 25.61 | 37.40±10.74 | - | - | - |
| Type F | 68.82 | 72.60 | 84.70±11.69 | 70.96 | 78.02 | 101.75±11.94 |
| Type G | 55.53 | 59.59 | 65.70±11.31 | 87.14 | 90.32 | 90.13±12.17 |
| Type H | 60.21 | 64.85 | 71.40±11.43 | 89.60 | 94.18 | 107.37±12.14 |
| Type I | 33.90 | 36.95 | 40.83±10.81 | 36.72 | 39.20 | 43.72±10.87 |
| Type J | 36.28 | 39.23 | 39.12±10.78 | 35.87 | 37.93 | 55.27±11.10 |
| Type K | 53.09 | 56.73 | 61.69±11.23 | 59.99 | 62.73 | 61.69±11.23 |

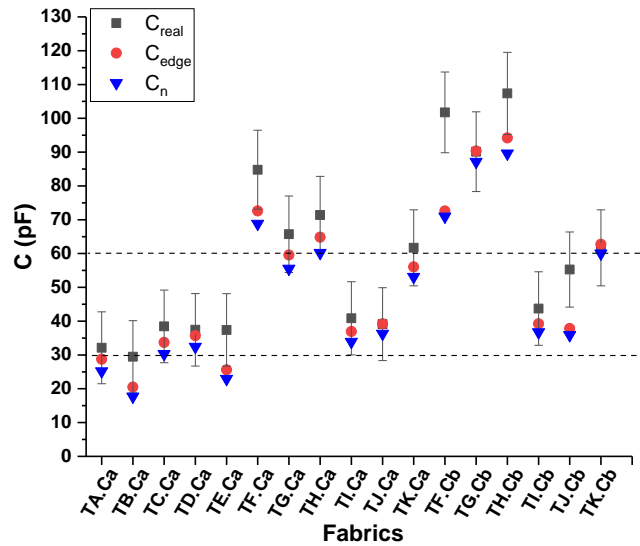


Figure 26. Graphical representation of the values of Table 16 related to the admitted limit of capacity.

Figure 27 shows the studied fabrics ordered by real capacity (from lowest to highest). The table can help in a capacitor design, allowing the choice of the type of fabric, more suitable for the desired capacitive sensor, with one or two sides of polyurethane

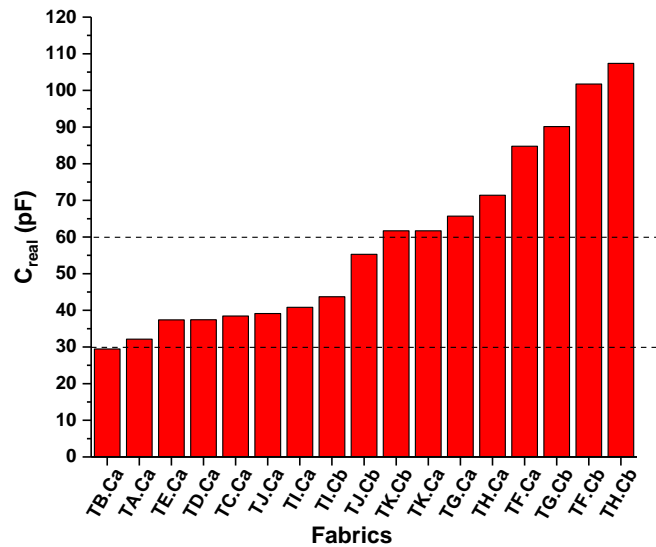


Figure 27. Real value of capacity ordered from lowest to highest for the type of fabric and number of polyurethane layers.

Conclusions

The development of sensors based on capacitive technologies must consider the parameters that most influence in the value of its capacity, permittivity and thickness are mainly provided by the fabric. Regarding the permittivity, since it has a direct relation with the value of the capacity, the fabric should have a low value. From the studied fabrics, those with polyester in their composition had a lower permittivity (below 2). With respect to the thickness, since it has an inverse relation with the value of the capacity, the fabric should have higher thicknesses; the problem is that the higher the thickness, the higher the rugosity and, hence, a greater difficulty for the correct printing of the conductive inks. The fabrics with thicknesses lower than 300 μm , a thread count higher than 40 threads/ cm^2 and a R_a lower than 25 μm , presented a higher easiness for the printing of the conductive inks. But these fabrics presented a problem of absorption of the conductive ink, implying that both sides were conductive and

avoiding the generation of a capacitive sensor. The use of dielectric inks to improve the rugosity and to create an isolating layer on lower thickness fabrics, did not give good results. They could improve the value of permittivity or the value of thickness, but they did not provide any benefit to improve the printing of conductive inks. On the contrary, the use of heat sealed polyurethanes improved noticeably the printing of conductive inks, and, in addition, improved the permittivity of the set and incremented the final thickness of the layer. As a disadvantage, it was necessary an additional stage to the sensor manufacturing process with specific equipment for the heat sealing. The set fabric-polyurethane presented, in some cases, the disadvantage of the lack of adhesion between them.

The conductive inks have a very low influence on the value of the sensor capacity, but their characteristics are fundamental when creating the plates of the capacitive sensor. The inks with very low viscosity and high solid content are the most optimal for this type of applications, since they penetrate between the threads of the fabrics and increment the conductivity of the conductor section. The printing direction of these inks in function of the warp and the weft also influenced in the final result of the capacity obtained. This factor will depend on the type of fabrics and its composition, but in general it is preferable the printing in the direction of the warp.

After considering all the variables studied, capacitive sensors below 60 pF have been obtained. Some of them had capacitive values close to 30 pF, recommended for this type of sensor. The calculation of the theoretical values gave results very similar to the real values obtained, allowing to determine all the parameters of the design before printing the sensor, saving time of development.

Declaration of conflicting interests

The authors declared no potential conflicts of interest with respect to the research, authorship and/or publication of this article.

Funding

The work presented is funded by the Conselleria d'Economia Sostenible, Sectors Productius i Treball, through IVACE (Instituto Valenciano de Competitividad Empresarial) and cofounded by ERDF funding from the EU. Application No.: IMAMCI/2019/1. This work was also supported by the Spanish Government/FEDER funds (RTI2018-100910-B-C43) (MINECO/FEDER).

References

- [1] Das, S. C., & Chowdhury, N. (2014). Smart textiles: New possibilities in textile engineering. *Journal of Polymer and Textile Engineering*, 1(1), 1-4.
- [2] Gonçalves, C., Ferreira da Silva, A., Gomes, J., & Simoes, R. (2018). Wearable e-textile technologies: A review on sensors, actuators and control elements. *Inventions*, 3(1), 14. doi:10.3390/inventions3010014.
- [3] Gehrke I, Tenner V, Lutz V, Schmelzeisen D, Gries T. *Sensor and Production Technologies for Industrial Smart Textiles Smart Textiles Production*. 2019. ISBN 978-3-03897-497-0. doi:10.3390/books978-3-03897-498-7.
- [4] Mostafalu, P., Tamayol, A., Rahimi, R., Ochoa, M., Khalilpour, A., Kiaee, G., ... & Sonkusale, S. R. (2018). Smart bandage for monitoring and treatment of chronic wounds. *Small*, 14(33), 1703509. doi: 10.1002/smll.201703509.
- [5] Molinaro, N., Massaroni, C., Presti, D. L., Saccomandi, P., Di Tomaso, G., Zollo, L., ... & Schena, E. (2018, July). Wearable textile based on silver plated knitted sensor for respiratory rate monitoring. In *2018 40th Annual International Conference of the IEEE Engineering in Medicine and Biology Society (EMBC)* (pp. 2865-2868). IEEE. doi:10.1109/EMBC.2018.8512958.
- [6] Ferraro, V. (2015, December). Smart textiles and wearable technologies for sportswear: a design approach. In *2nd International Electronic Conference on Sensors and Applications*. Multidisciplinary Digital Publishing Institute. doi:10.3390/ecsa-2-S3005.
- [7] Shi, H., Zhao, H., Liu, Y., Gao, W., & Dou, S. C. (2019). Systematic Analysis of a Military Wearable Device Based on a Multi-Level Fusion Framework: Research Directions. *Sensors*, 19(12), 2651. doi:10.3390/s19122651.
- [8] Costa, R., Oliveira, P., Grilo, A., Schwarz, A., Cardon, G., DeSmet, A., ... & Pomazanskyi, A. (2017, June). SmartLife smart clothing gamification to promote energy-related behaviours among adolescents. In *2017 International Conference on Engineering, Technology and Innovation (ICE/ITMC)* (pp. 1489-1495). IEEE. doi:10.1109/ICE.2017.8280058.
- [9] Mann, G., & Oatley, G. (2017, April). Positive design of smart interactive fabric artifacts for people with dementia. In *2017 IEEE 5th International Conference on Serious Games and Applications for Health (SeGAH)* (pp. 1-8). IEEE. doi:10.1109/SeGAH.2017.7939257.
- [10] Andonovska, M. (2009). *E-textiles: The Intersection of Computation and Traditional Textiles* (Doctoral dissertation, Yüksek Lisans Tezi, Medialogy, Aalborg University, Copenhagen. Birkhauser).

- [11] Wang, Q., Chen, W., & Markopoulos, P. (2014, May). Smart garment design for rehabilitation. In *ICTs for Improving Patients Rehabilitation Research Techniques* (pp. 260-269). Springer, Berlin, Heidelberg.
- [12] Kim, K., Jung, M., Jeon, S., & Bae, J. (2019). Robust and scalable three-dimensional spacer textile pressure sensor for human motion detection. *Smart Materials and Structures*, 28(6), 065019. doi:10.1088/1361-665X/ab1adf.
- [13] Ferri, J., Perez Fuster, C., Llinares Llopis, R., Moreno, J., & Garcia-Breijo, E. (2018). Integration of a 2D Touch Sensor with an Electroluminescent Display by Using a Screen-Printing Technology on Textile Substrate. *Sensors*, 18(10), 3313. doi:10.3390/s18103313.
- [14] De Vos, M., Torah, R., Glanc-Gostkiewicz, M., & Tudor, J. (2016). A complex multilayer screen-printed electroluminescent watch display on fabric. *Journal of Display Technology*, 12(12), 1757-1763. doi:10.1109/JDT.2016.2613906.
- [15] Lin, X., & Seet, B. C. (2016). Battery-free smart sock for abnormal relative plantar pressure monitoring. *IEEE transactions on biomedical circuits and systems*, 11(2), 464-473. doi:10.1109/TBCAS.2016.2615603.
- [16] Ejupi, A., & Menon, C. (2018). Detection of Talking in Respiratory Signals: A Feasibility Study Using Machine Learning and Wearable Textile-Based Sensors. *Sensors*, 18(8), 2474. doi:10.3390/s18082474.
- [17] Polanský, R., Soukup, R., Řeboun, J., Kalčík, J., Moravcová, D., Kupka, L., ... & Hamáček, A. (2017). A novel large-area embroidered temperature sensor based on an innovative hybrid resistive thread. *Sensors and Actuators A: Physical*, 265, 111-119. doi:10.1016/j.sna.2017.08.030.
- [18] Komazaki, Y., & Uemura, S. (2019). Stretchable, Printable, and Tunable PDMS-CaCl₂ Microcomposite for Capacitive Humidity Sensors on Textiles. *Sensors and Actuators B: Chemical*, 126711. doi:10.1016/j.snb.2019.126711.
- [19] Ng, C. L., & Reaz, M. B. I. (2019). Evolution of a capacitive electromyography contactless biosensor: Design and modelling techniques. *Measurement*. doi:10.1016/j.measurement.2019.05.031.
- [20] Ferri, J., Lidón-Roger, J., Moreno, J., Martinez, G., & Garcia-Breijo, E. (2017). A wearable textile 2D touchpad sensor based on screen-printing technology. *Materials*, 10(12), 1450. doi:10.3390/ma10121450.
- [21] Atalay, O. (2018). Textile-based, interdigital, capacitive, soft-strain sensor for wearable applications. *Materials*, 11(5), 768. doi:10.3390/ma11050768.
- [22] Du, L. (2016). An overview of mobile capacitive touch technologies trends. *arXiv preprint arXiv:1612.08227*.
- [23] Bhalla, M. R., & Bhalla, A. V. (2010). Comparative study of various touchscreen technologies. *International Journal of Computer Applications*, 6(8), 12-18.
- [24] Gu H., Sterzik C. (2013). Capacitive Touch Hardware Design Guide. *MSP430 Texas Instruments*.
- [25] Salim, A., & Lim, S. (2017). Review of recent inkjet-printed capacitive tactile sensors. *Sensors*, 17(11), 2593. doi:10.3390/s17112593.

- [26] Sergio, M., Manaresi, N., Tartagni, M., Guerrieri, R., & Canegallo, R. (2002). A textile based capacitive pressure sensor. In *SENSORS, 2002 IEEE* (Vol. 2, pp. 1625-1630). IEEE. doi: 10.1109/ICSENS.2002.1037367.
- [27] Kim, Y., Kim, H., & Yoo, H. J. (2009). Electrical characterization of screen-printed circuits on the fabric. *IEEE transactions on advanced packaging*, 33(1), 196-205. doi:10.3390/fib7060051.
- [28] Lee, W. J., Park, J. Y., Nam, H. J., & Choa, S. H. (2019). The development of a highly stretchable, durable, and printable textile electrode. *Textile Research Journal*, doi:10.1177/0040517519828992.
- [29] Chatterjee, K., Tabor, J., & Ghosh, T. K. (2019). Electrically Conductive Coatings for Fiber-Based E-Textiles. *Fibers*, 7(6), 51. doi:10.3390/fib7060051.
- [30] Gu, J. F., Gorgutsa, S., & Skorobogatiy, M. (2010). Soft capacitor fibers using conductive polymers for electronic textiles. *Smart Materials and Structures*, 19(11), 115006. doi:10.1088/0964-1726/19/11/115006.
- [31] Hagan, M., & Teodorescu, H. N. (2013, November). Intelligent clothes with a network of painted sensors. In *2013 E-Health and Bioengineering Conference (EHB)* (pp. 1-4). IEEE. doi:10.1109/EHB.2013.6707390.
- [32] Khan, S., Lorenzelli, L., & Dahiya, R. S. (2014). Technologies for printing sensors and electronics over large flexible substrates: a review. *IEEE Sensors Journal*, 15(6), 3164-3185. doi: 10.1109/JSEN.2014.2375203.
- [33] Mukherjee, P. K. (2019). Dielectric properties in textile materials: a theoretical study. *The journal of the Textile Institute*, 110(2), 211-214. doi:10.1080/00405000.2018.1473710.
- [34] Fischer, D. (2010). Capacitive Touch Sensors: Application Fields, Technology Overview, and Implementation Example. *Fujitsu Microelectronics Europe*.
- [35] (2016, September). PCF8883: Capacitive touch/proximity switch with auto-calibration, large voltage operating range, and very low power consumption. *NXP Semiconductors*.